In presenting the dissertation as a partial fulfillment of the requirements for an advanced degree from the Georgia Institute of Technology, I agree that the Library of the Institution shall make it available for inspection and circulation in accordance with its regulations governing materials of this type. I agree that permission to copy from, or to publish from, this dissertation may be granted by the professor under whose direction it was written, or, in his absence, by the dean of the Graduate Division when such copying or publication is solely for scholarly purposes and does not involve potential financial gain. It is understood that any copying from, or publication of, this dissertation which involves potential financial gain will not be allowed without written permission.

AN INVESTIGATION OF THE DYNAMIC BEARING CAPACITY OF FOOTINGS ON SAND

A THESIS

Presented to

the Faculty of the Graduate Division

by

John Marvin Woodard

In Partial Fulfillment

of the Requirements for the Degree

Master of Science in Civil Engineering

Georgia Institute of Technology

April, 1964

AN INVESTIGATION OF THE DYNAMIC BEARING CAPACITY

OF FOOTINGS ON SAND

Approved:

Chairman

Date approved by Chairman June 8, 1964

ACKNOWLEDGMENTS

My sincere thanks are due Dr. Aleksandar S. Vesić for his dedicated assistance in conducting the investigation and for his aid in preparation of this text. The author is also most grateful to Professors George F. Sowers and Austin B. Caseman for their beneficial comments on this text.

TABLE OF CONTENTS

LIST OF TABLES

LIST OF ILLUSTRATIONS

SUMMARY

The purpose of this investigation was to determine the effect of a variation in load rate on the bearing capacity of a surface footing on sand. A total of 29 tests on both dry and saturated sand were conducted.

Dense sand models were constructed in a test box and a four-inch diameter circular steel footing was hydraulically loaded on the surface of the sand.

The hydraulic loading device was controlled by a system of manual and solenoid valves which could control the rate of loading in a range of about 12.3 inches per second to 0.000023 inches per second. Continuous plots of settlement and load versus time were provided by a Sanborn Recorder. Density of each model was determined by a static cone penetrometer.

The results of tests on dry sand show a minimum bearing capacity at a load rate of about 0.002 inches per second. At load rates decreasing from this value, the bearing capacity increases by a maximum of 37.5 per cent. For load rates increasing from 0.002 inches per second, the bearing capacity increases by a maximum of 29.0 per cent of the minimum value. All tests in dry sand exhibited a complete bearing capacity failure with the rupture surface intercepting the sand surface.

Tests on saturated sand show the same general trend as those on dry sand, except to a much greater magnitude. The minimum bearing capacity existed at a load rate of 0.002 inches per second. For load rates slower than this value, the bearing capacity increased 65.0 per cent.

Increasing load rates produced an increase in bearing capacity to approximately three times this minimum value. The general shape of the curve representing the comparison of bearing capacity and load rate is similar for dry and submerged sand except for load rates greater than about 0.3 inches per second. For load rates faster than this value, the bearing capacity for footings on submerged sand increases very rapidly, while there is only a slight increase for footings on dry sand.

CHAPTER I

INTRODUCTION

The advent of large ground disturbances and overpressure on structures and their foundations caused by nuclear blasts has in the last few years exposed the lack of adequate understanding of the behavior of soils under these dynamic conditions. Several investigations have been made through the years, but studies of the behavior of soil under vibratory loads have been mainly stressed. The work presented here deals with the equally important problem of transient loads. These are loads applied at a higher rate of strain than about one per cent per minute.

Of the small amount of work done in this area of study, most investigations were made with samples tested in triaxial apparatus. Early works along this line were the studies of Casagrande and Shannon (1, 2) and Whitman (3, 4, 5). Casagrande and Shannon found an increase of approximately 15 per cent in the failure load on sands existed for a variation in time to failure from 2000 seconds to 0.02 seconds. Also reported was an increase in the modulus of deformation for an increase in load rate. Whitman reported the same trend with an increase of 10 to 15 per cent in strength of triaxial samples when the load rate was increased from a "normal slow test" to a load rate which produced failure in a few hundred microseconds. In more recent tests, Whitman states that the variation in the angle of internal friction is not more than ten per cent and probably less than five per cent for a range of five minutes to five milli-

seconds until failure. Neglecting dilatancy, Seed and Lundgren (6) found an increase of 15 to 20 per cent in triaxial sample strength of saturated, dense sand specimens as the load rate was increased from that for static tests to 40 inches per second. Including dilatancy, the strength increase was reported to be 40 per cent with about half attributed to negative porewater pressure due to dilatancy and half due to the effect of high rates of load on strength. Also reported was a 30 per cent increase in the modulus of deformation for strain rates increasing from static tests to load rates of 40 inches per second. A few tests have been performed on small-size model footings. DeBeer and Vesić (7) noted a decrease in bearing capacity for increased rates of loading on rectangular footing, two inches by 12 inches, placed on sand. These tests were performed at rates of loading in the range of about 0.00001 inches per second to 0.0001 inches per second. This is consistent with the work presented here, since for the same range of loading rates a decrease in bearing capacity was also found.

Besides the tests mentioned here, work is being performed at the Waterways Experiment Station, the Armour Research Foundation, the University of Illinois, and the Naval Civil Engineering Laboratory. Other results of bearing capacity tests on small footings have been published (8, 9, 10, 11, 12, 13).

At the present time, the amount of information in this field is rather limited. The author presents in this work the results of tests on a four inch circular footing located on the surface of both dry and saturated sand. Rates of loading covering practically the entire range of transient loads were used. The range extended from a rate of 12.3

inches per second to 0.000023 inches per second. All loads were applied with the same hydraulic apparatus and continuous plots of load-time and deflection-time were recorded.

CHAPTER II

EQUIPMENT AND PROCEDURE

Construction of Models

As used in this discussion, the term "model" refers to both the footing and the sand beneath it. Placement of the sand and footing, along with the densification of the sand, will be referred to as construction of the model. Two construction procedures, one for the wet tests and one for the dry tests, were developed with the purpose of obtaining as much homogeneity as possible with respect to density. The method of construction for dry tests was vibratory compaction, while for wet tests a combination of rolling and vibratory methods was employed.

Equipment

The following equipment was used in the model construction:

(1) dry sand,

(2) a steel, water proof test box with provision for introducing water,

(3) containers for handling the sand, both to and from the box,

(4) two steel plates with vibrators attached,

(5) a footing, and

(6) a concrete roller.

The sixth item was used only for construction of the wet tests. In the following discussion, each of these items will be discussed in detail, as will construction methods for both dry and wet tests.

Sand

Chattahoochee River sand, sieved through a window screen with openings slightly greater than a standard number 16 sieve, was used in all tests. The grain-size distribution curve is shown in Figure 1. Tests resulted in a minimum density of 79.0 lb. per ft.^{3} and maximum density of 102.5 lb. per ft.^{3}. It may be described as a medium, uniform, subangular micaceous sand. For the dry tests, the moisture content was determined to be 0.1 per cent. Figure 2 presents the angle of internal friction, ϕ, as a function of the void ratio, e, as determined by Duncan (14).

Steel Box

Models were constructed in a steel box 50 inches square and 70 inches deep. One side of the box has two doors, one above the other, which were sealed water-tight. All side and bottom seams of the box were also made water-tight by welding. Near one bottom corner of the box a pipe for filling with water and a drain were installed. The drain was well screened to prevent loss of sand during draining. A 30-inch piezometer was placed on one side of the box to measure the water level in the sand. The model box is shown in Figure 3. Markings were drawn horizontally along the inside of the box every four inches to aid in sand placement.

Sand Containers

A two feet square, two feet deep steel box with a bottom sloping to a six inch opening was used to transport the sand in and out of the steel test box between dry tests. The sand container was placed on a fork-lift truck and raised into the proper position for either filling or emptying the test box. The sand was removed from the test pit by

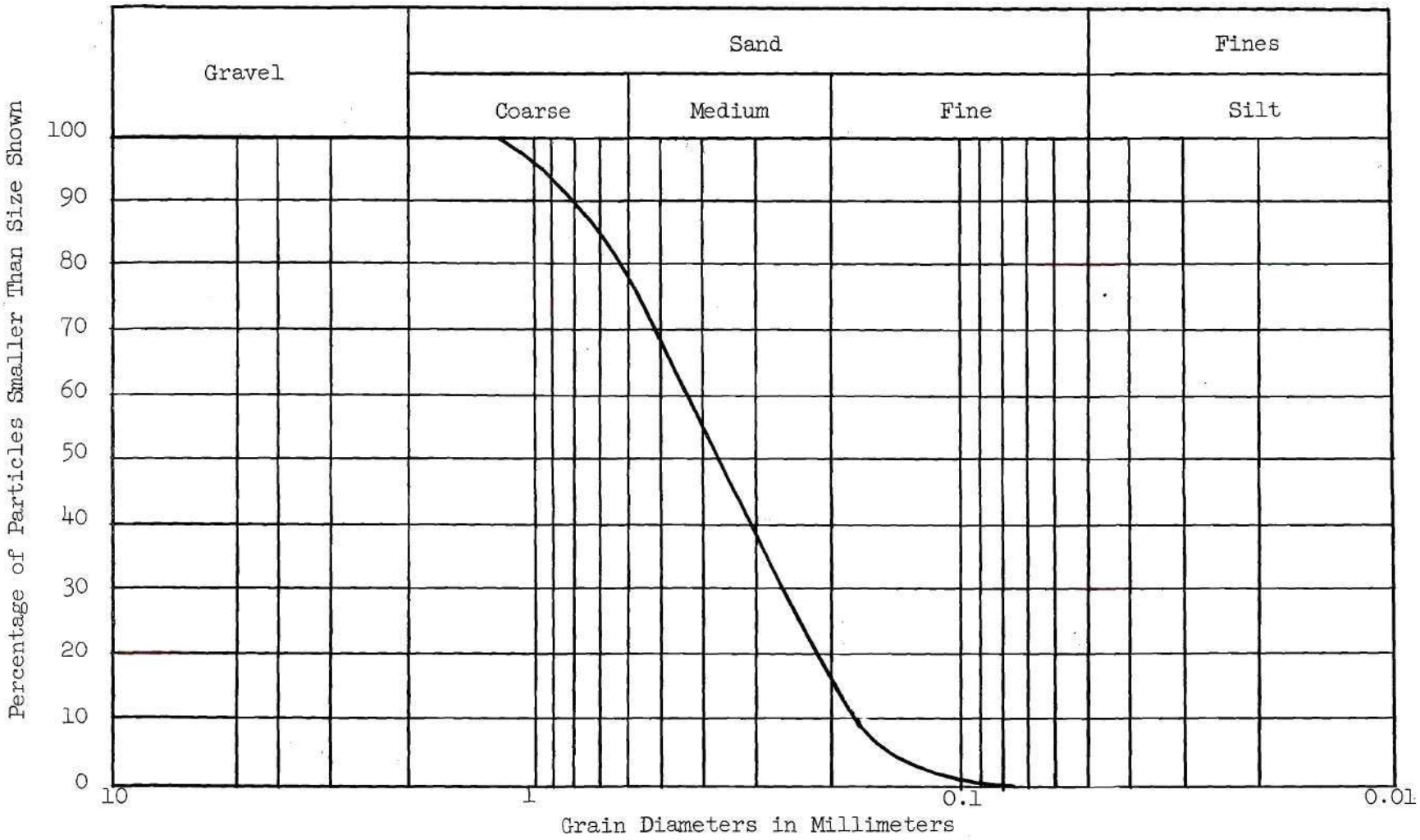

Figure 1. Grain-Size Distribution Curve.

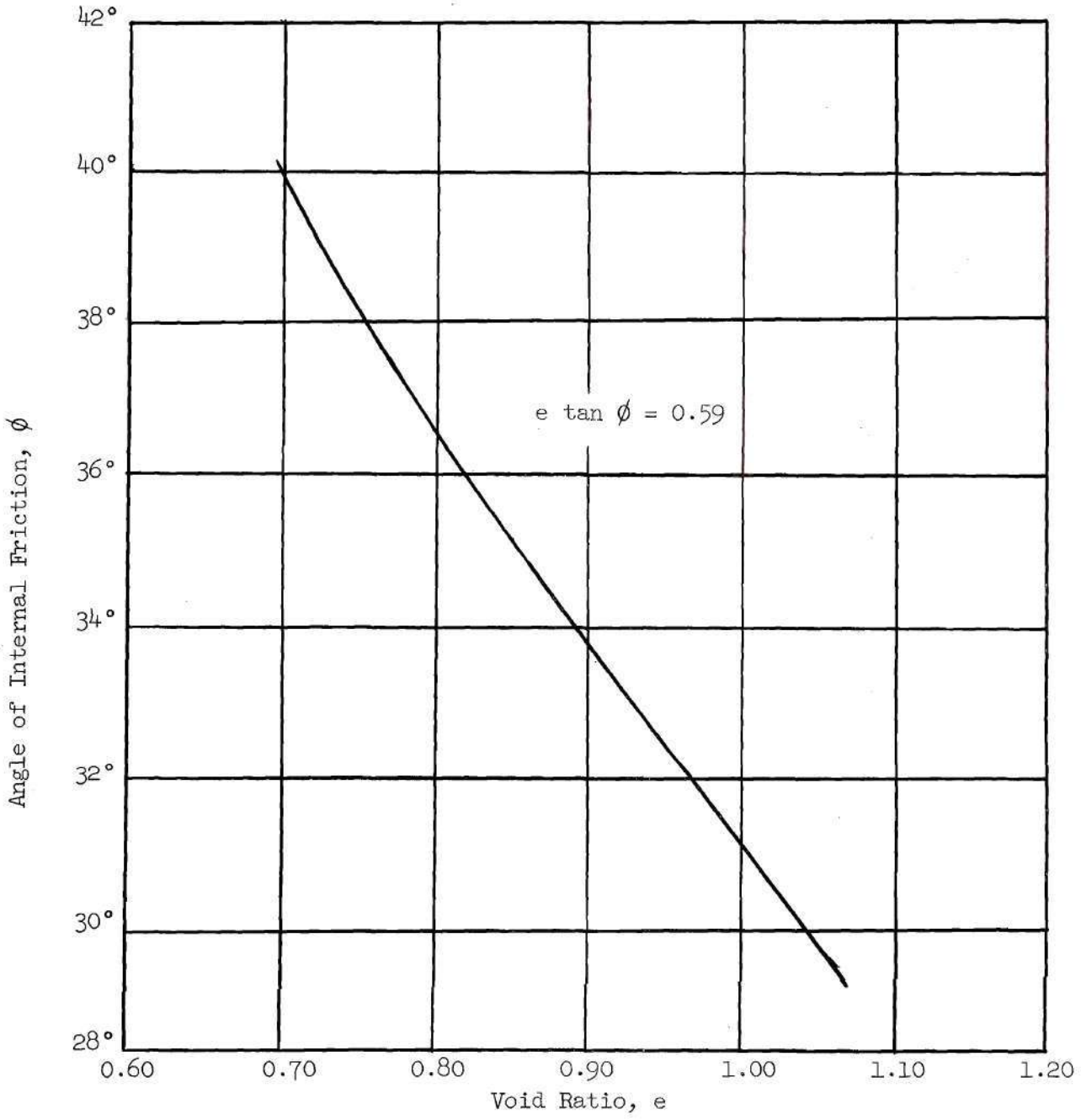

Figure 2. Angle of Internal Friction as a Function of Void Ration.

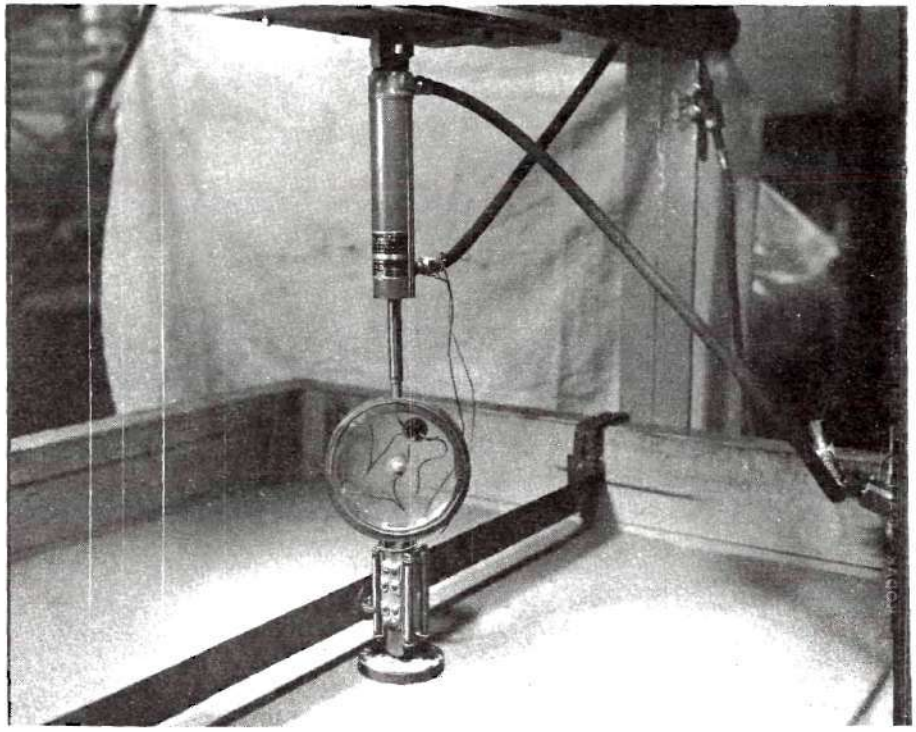

Figure 3. Test Area

hand, but was replaced by operating a manual valve on the sand container allowing it to free fall back into the test box.

For the wet tests, a platform ten feet by five feet was erected near the test box and the sand was manually moved between the test box and this platform.

Vibrator Plates

Two Syntron Electric Vibrators were bolted at the centers of two 24 inch by 48 inch, 1/4 inch thick steel plates. Each plate and vibrator weighed 120 pounds. The frequency of the vibrators was 60 cycles per second and the amplitude about 1/32 inch for the dry tests. It was found that the amplitude was somewhat dampened during the wet tests.

Footing

The footing was a circular steel plate 1/2 inch thick and four inches in diameter. Coarse sandpaper was attached with a rubber base glue to the under side on the footing to provide a rough interface between the footing and the sand. This was replaced after each wet test due to deterioration of the sand paper by water. A small circular indentation was machined into the center of the top of the footing which provides a seat for the loading mechanism. The loading mechanism was rounded to fit perfectly this indentation to prevent any moment on the footing from developing.

Concrete Roller

In construction of the wet models, a 30 pound, 6 inch diameter, 12 inches long concrete cylinder was used to roll each lift of damp sand before vibration proceeded.

Model Construction

Dry Tests

After each test the sand was manually removed to a depth of 20 inches from the surface. Twenty inches was chosen since this is below the zone of influence of the previous test. The sand was placed in the two feet by two feet steel box and lowered by use of a fork-lift truck. This sand was stored in 55 gallon steel drums.

The surface was leveled by use of a wooden straight edge and vibrated for three minutes to restore the sand to the proper density. This three-minute vibration period was based on previous experience with both the same vibrator plates and sand.

Sand was randomly deposited over the previously vibrated surface until a depth of four inches was reached. The surface was leveled using the horizontal markings on the test box as a guide. This surface was vibrated for three minutes, during which time the two plates were held together to prevent the formation of a less dense zone between them. Each four-inch lift was constructed in this manner, with the plates being rotated 90 degrees after each vibration to help insure better uniformity.

Wet Tests

The construction of the models using wet sand was similar to that of those using dry sand except that several problems were encountered which made it more difficult to control the density.

First, the sand was moist when placed into the test box and was in a bulked condition, making it very loose.

Second, once the sand had been vibrated and the plates removed the water pressure due to the upward flow of water caused the voids to expand, decreasing the density.

The following modifications to the procedure used in dry test model construction were introduced to overcome these difficulties: After removing the wet sand the prescribed 20 inches, the water table was lowered four inches below the sand surface. The surface was leveled and then rolled with the concrete roller, one pass in each direction. This produced a density comparable to that of the dry sand immediately after placing and before vibration. The moist sand was then vibrated for two minutes, after which time the vibration was ceased and the water table raised to the sand surface. Another one minute of vibration followed with the sand submerged. By leaving the plates on the surface of the sand during inundation, and vibrating the sand saturated for one minute, the decrease in density due to the upward water flow was greatly eliminated.

Each successive four-inch layer was compacted in exactly the same manner, remembering that the water table is lowered four inches after each lift. This allows the plates to be removed more easily without disturbing the surface of the sand.

Testing

The equipment as described below was used in all tests without modification.

Equipment

The following equipment was used in testing a model:

(1) a proving ring,

(2) a set of resistance coils,

(3) a strip-chart recording device,

(4) a hydraulic system for loading the footing, and

(5) a penetrometer for determining model density.

Proving Ring

A proving ring with a mean diameter of 6.1 inches, a thickness of 0.6 inches, and a width of 1.0 inches was used to determine the load applied to the footing. Four SR-4 strain gages wired in a Wheatstone Bridge Circuit were mounted on the internal circumference of the ring and provided the change in signal transmitted to the recorder. The relationship between load and strain for the ring was linear up to the design load of 3000 pounds.

Tapped holes were provided in both the top and bottom of the proving ring on the vertical diameter to provide attachment between the loading column and the hydraulic loading cylinder. (See Figures 4,5, and 6). It is important to note here that with the proving ring in this position there is no need to account for the inertia forces of either the loading piston or hydraulic oil. The inertia of the footing and loading column do influence the loading, but the extent is very small.

Resistance Coils

Deformations of the footings were measured by the use of two 120 ohm wire coil resistors wired in parallel. These coils were attached to each side of the loading column and a bracket-shaped sliding contact was mounted so that the voltage drop from the bottom of the pair of coils to the contacts could be recorded and related to footing deflection. (See Figure 5 and 7).

Recording Device

All footing loads and deflections were recorded by a Sanborn Two

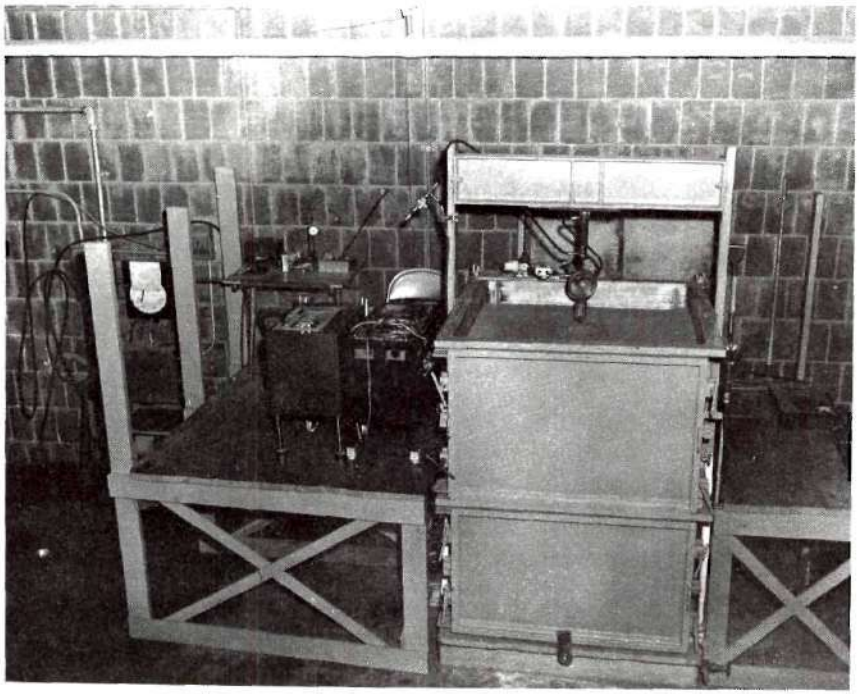

Figure 4. Loading Apparatus

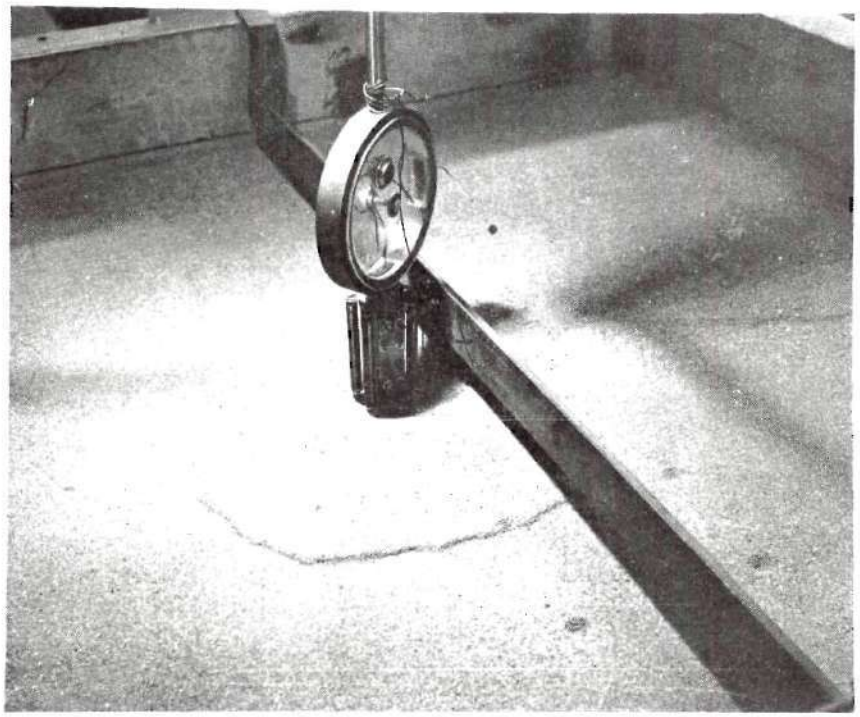

Figure 5. Sand Surface at Completion of Test

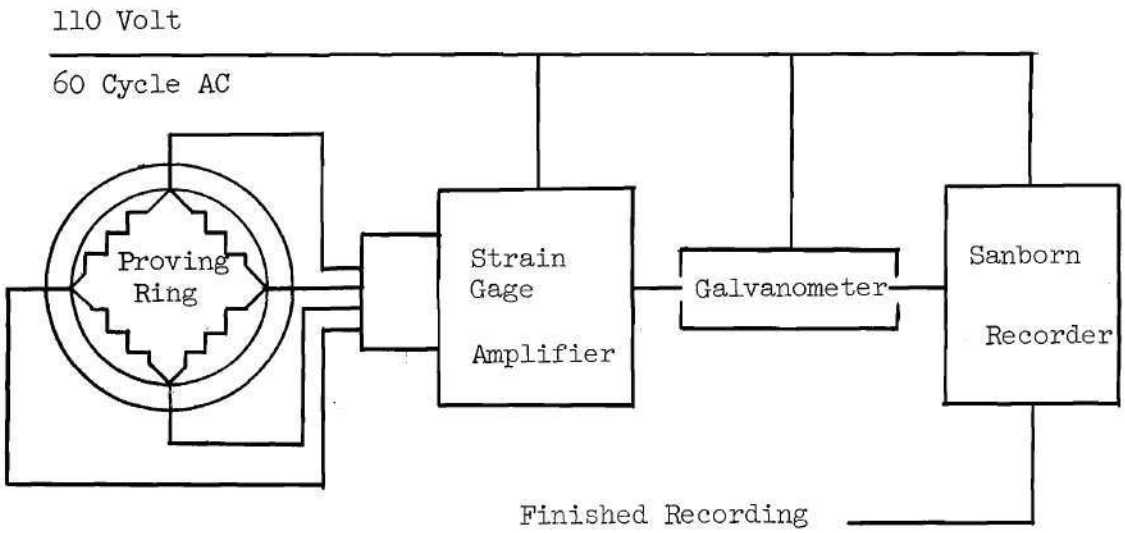

Figure 6. Basic Circuit for Measurement of Load

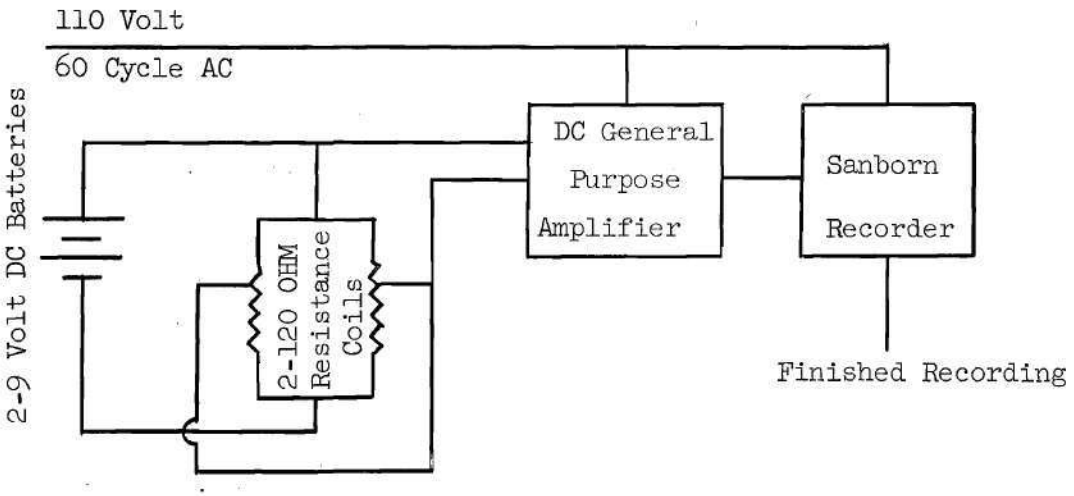

Figure 7. Basic Circuit for Measurement of Deflection.

Channel Recording Instrument, Model No. 60. This model was equipped with a timing device which recorded time along the abscissa with load and deflection along the ordinate. This instrument provided a convenient means of determining lapsed time, load rate, and time to failure.

A Sanborn DC General Purpose Amplifier, Model No. 64-300B, was used to amplify the voltage changes across the resistance coils. Settlements could be read with this instrument directly to 0.07 inches and estimated to 0.007 inches.

A Sanborn Strain Gage Amplifier, Model No. 64-500B, was used to record changes in resistance of the SR-4 strain gages in the proving ring. The sensitivity was such that load could be directly read to 11.1 pounds and estimated to 1.1 pounds.

Calibration of stylus deflection for both footing penetration and load were made after every third test to insure that no change had occurred.

Hydraulic Loading System

The loading system utilized the basic hydraulic system shown in Figure 8. A Bosch Fuel Injection Pump supplied oil from a 1 1/2-gallon reservoir to a one-gallon accumulator. The pump was driven by a 1/3 horsepower electric motor which was controlled by an electronic device which started the pump when the accumulator pressure dropped below the prescribed 1400 pounds per square inch (see Figure 9). A 3/8-inch, 3000 pounds per square inch hydraulic line carried the oil to the valving system. All lines in the valving system were 1/4-inch, 3000 pounds per square inch hoses. The valving system consisted of two parallel lines, each containing two valves.

The following valves were used:

(1) Valves 1 and 2 were flow control valves with a range of operation of from full-throat to about 2.5×10^{-4} cubic inches of oil per second.

(2) Valve 3 was a 115-volt, 60-cyclic, normally closed, 3000 pounds per square inch solenoid valve.

(3) Valves 4, 5, 6, and 7 were high pressure globe type valves.

A double acting hydraulic cylinder with a piston head diameter of 1 1/2 inches and six inches stroke was used to load the footings. This small diameter cylinder was chosen to insure high piston velocity. With an oil pressure of 1400 pounds per square inch, the maximum load obtainable was about 2480 pounds. Since the largest footing test load was only about 900 pounds, the system was overpowered by a factor of about 2.75. This insured smooth operation and eliminated piston lag due to friction.

Since oil was supplied at a constant pressure and rate, the piston moved at constant velocity for all slower tests. Testing at rates greater than five inches per second produced a drop in pressure of about 80 pounds per square inch. This was not noticeable in the results, however, due to the overpower factor in the system.

Penetrometer

A static cone penetrometer of 1/2-inch point connected to a 3/8-inch rod was used to determine model density. Two soundings were made at increments of one inch to a depth of 12 inches. A screw jack was employed to advance the penetrometer into the sand and the resistance encountered was measured by a proving ring.

The average resistance taken at each whole inch were averaged and reduced to density using the previously determined depth-penetration

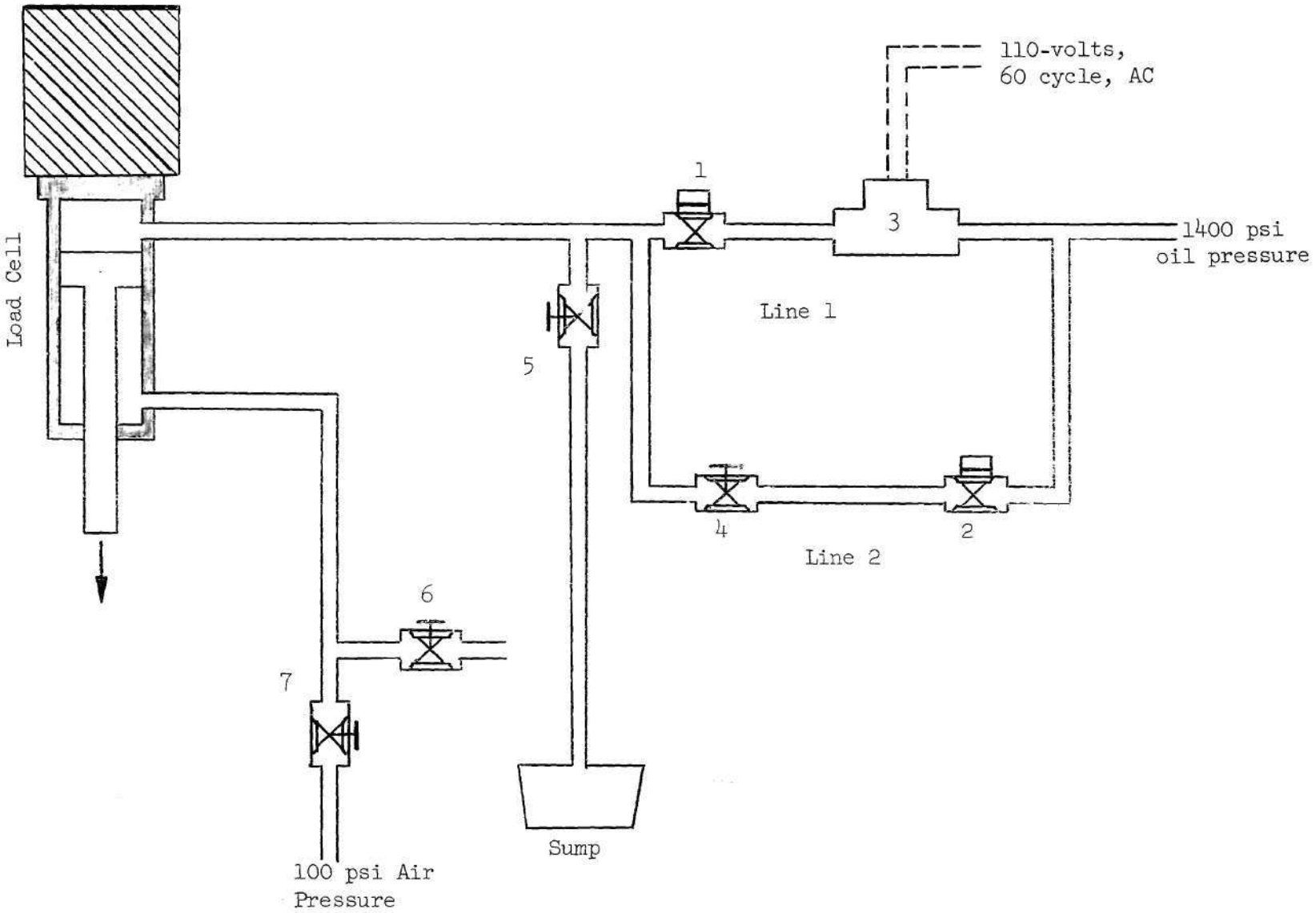

Figure 8. Flow Diagram of Valve System

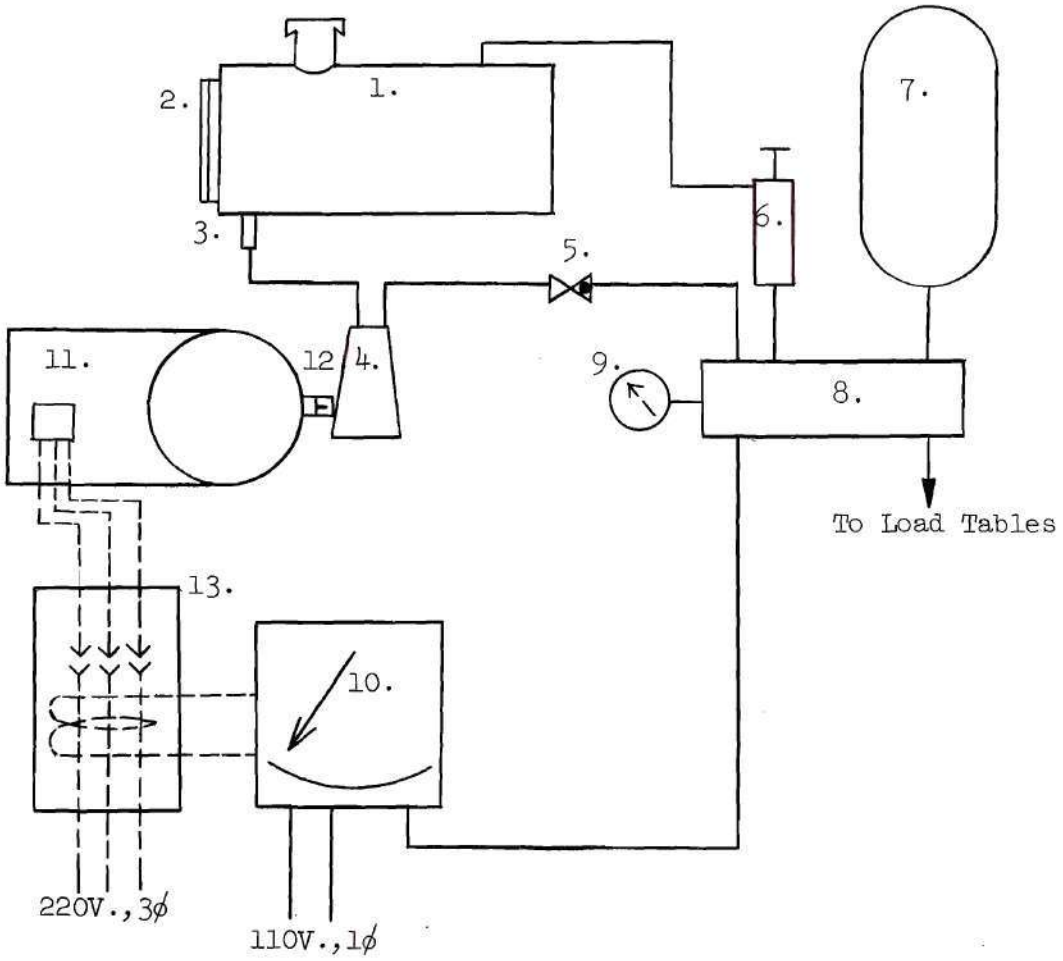

1. Reservoir, Vent to Atmosphere
2. Visual Oil Level Gage
3. Strainer
4. American-Bosch Fuel Injection Pump-APE 1B90P 300/3
5. Vickers In-Line Check Valve, 1/4 Pipe Size Model No. DT 8P1-02-68-10
6. Vickers Remote Control Pressure Relief Valve Model No. C-175-F-10
7. Greer 1 Gallon, 30A-1A Hydraulic Accumulator, 3000 psi Series, Nitrogen Charged
8. Manifold
9. Pressure Gage
10. Minneapolis-Honeywell, Electrovane Pressure Controller, Indicating Type, 1250-2500 psi, Model MH 704 CIP2-23 111 IV H
11. Boston Gear Ratiomotor No. M 115-30 EW with 1/3 HP, 220 V, 3ϕ Electric Motor
12. Boston Gear Coupling FC BB 15
13. Magnetic Holding Coil, 3 Pole, Normally Open, 30 Amp Switch

Figure 9. Hydraulic Pumping System

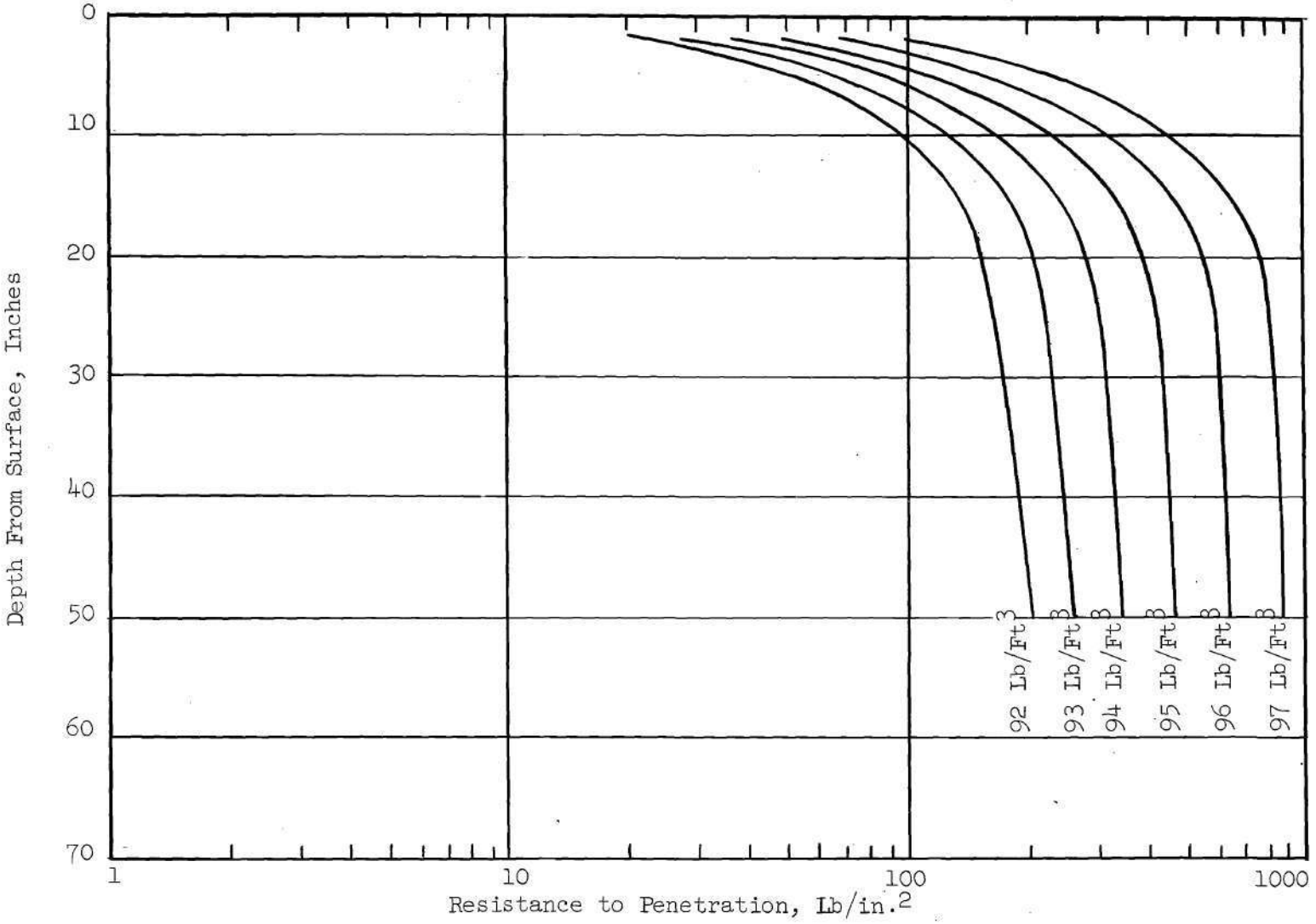

Figure 10. Penetrometer Resistance as a Function of Depth for Several Densities.

resistance density relationship shown in Figure 10. The model density was taken as the average density of the first 12 inches.

A correction factor was applied to all soundings made during the wet tests. Since the sand was submerged, the unit weight was less and all resistances to penetration of the static cone were less. All resistances were corrected by multiplying them by the ratio of dry unit weight to submerged unit weight. This term can be reduced to $\frac{G}{G-1}$ and was taken as 1.6 in all wet tests.

Loading the Footing

After completion of compaction of the last lift of sand, the loading columm, resistance coils, and proving ring were connected to the piston shaft of the hydraulic cylinder. An amount of oil was introduced into the cylinder until contact was made between the loading column and the footing. The sliding contact brackets were placed in position and wired to the batteries.

After a 30 minute warm-up period, the Sanborn recording instrument was connected to the coil and proving ring.

Footings were tested using either line 1 or line 2 depending on the rate of load desired. For rates of loading greater than 0.2 inches per second, line 1 was used in the following manner:

1. Close valves 2, 4, 5 and 7.
2. Open valve 1 the desired amount and then open valve 6.
3. Electrically activate valve 3, thus loading the footing.
4. After completion of test, deactivate valve 3 and close valves 1 and 6.

5. Open valves 5 and 7 to return piston to original position and by-pass used oil to sump.

For rates of loading less than 0.2 inches per second, line two was used in the following manner:

1. Close valves 1, 5, and 7.
2. Open valve 2 the desired amount and then open valve 6.
3. Open valve 4 to load the footing.
4. After completion of test, close valves 2, 4, and 6.
5. Open valves 5 and 7 to return piston to original position and by-pass used oil to sump.

The correct setting of the flow control valves was determined by constructing a line on the recorder paper at the desired slope representing load rate. By slight changes in the flow-control valve settings, the Sanborn recording stylus representing deflection was made to follow this pre-set line.

After each test was completed, air pressure returned the piston to its original position.

CHAPTER III

DISCUSSION OF RESULTS

All relationships pertaining to time were obtained from the recorded settlement-time and load-time curves. The values for "time to failure" and "time of test" for each test were obtained in this manner. Also, from these continuous curves, the load settlement relationship for each test was determined and plotted (see Figures 11 through 20). From these deduced curves, a criterion for failure was established. For dry sands and for the wet tests conducted at slower loadings, the load settlement curves all had the same general shape. Each curve had an initial linear section which after reaching a maximum load decreased to some smaller load at which point the load increased again (see Figure 21). The criterion for failure load for such curves was the maximum load reached at the first peak. Settlement at failure is taken as the settlement corresponding to the failure load. The time to failure is the time required to reach the failure load and the load rate is the total settlement of the footing divided by the total time of the test.

The variation of percentage of settlement (failure settlement per footing width times 100) at failure with load rate is shown in Figure 22. For dry tests, the plots indicate an increase from 4.2 per cent at 0.000023 inches per second to a constant value of 8.2 per cent. At about one inch per second, the percentage again increases at a rapid rate to a maximum of about 13.5 per cent at ten inches per second. Vesić (15) reported a percentage of failure settlement of about eight per cent for

circular footings loaded on the surface of a sand with a dry unit weight of 97.0 lb/ft^3 at a rate of loading which produced failure in about 20 minutes.

A somewhat different type of load settlement curve existed for the faster wet tests (see Figure 23). The load-settlement curve for these tests never reached a peak value, but continued to increase until the maximum deflection of the hydraulic system was achieved.

The failure load for these tests was obtained by two different methods. The first method was based on a load bearing criterion and disregarded the magnitude of settlement at failure. The failure load was obtained by constructing a graph of the slope of the load-settlement curve $(\frac{dp}{d\delta})$ at chosen points versus the corresponding settlements. The failure load was taken as the point on this curve where the slope $(\frac{dp}{d\delta})$ is approaching some constant value. The load corresponding to this failure point was obtained from the load-settlement curve and designated the failure load with the settlement at this point becoming the settlement at failure (see Figure 24). Settlements at failure based on this method of failure definition are extremely high and reach approximately 40 per cent of the footing width.

The second method of defining failure was based on a settlement criterion. Ratios of settlement at failure versus footing width (B) were compared with the load rates; they are shown in Figure 22. For wet tests, the percentage failure settlement increased from a value of 2.5 per cent at 0.0001 inches per second at a slightly decreasing rate to about 6.2 per cent at 0.02 inches per second load rate. At this point, the percentage increased sharply at a very steep rate to a maximum of about 40 per cent,

if failure is based on the load-bearing criterion of method one. However, if settlement is taken as the criterion for failure, it is more reasonable to believe that the percentage settlement should increase at a much slower rate corresponding to the trend experienced for dry tests. Therefore, taking a failure criterion based on settlement, the dashed line branching at about 0.3 inches per second from the wet test plot of percentage failure settlement represents failure. Obtaining values of failure settlement from this line, the failure loads for tests 13, 14, 19, 20, and 21 were obtained from their load-settlement curves (see Table 1). Figure 26 shows the plot of $\frac{Qult}{1/2\gamma B}$ versus load rate as a dashed line for wet tests conducted at rates of load greater than 3.6 inches per second and based on a settlement criterion of failure.

Two characteristic types of failure were observed in testing. The first type of failure was a sudden drop in bearing resistance accompanied by the appearance of failure shear surfaces intercepting the sand surface. This type of failure was experienced in all dry tests and all wet wet tests conducted at load rates less than 3.6 inches per second. Figure 25 shows the distances from the center of the footing to the shear surface for dry tests. Considerable bulging of the area around the footing accompanied the appearance of the shear surface (see Figure 5). This type of failure is described by Terzaghi, it is termed "general shear" failure (16).

The second type of failure was experienced for wet tests performed at load rates greater than 3.6 inches per second. No shear surfaces were observed and only a small amount of bulging directly next to the footing was noticed. This type of failure is of the same nature

Table 1. Loads at Failure Based on Settlement Criterion of Failure

Test	Ratio Failure Settlement to Footing Width Per Cent	Settlement at Failure in.	Failure Load lb.	$\frac{(Q_{ult})}{1/2\gamma B}$
29	13.8	0.552	264	307
26	12.3	0.492	540	615
28	13.5	0.540	560	638
27	13.3	0.532	425	483
25	11.6	0.464	430	490

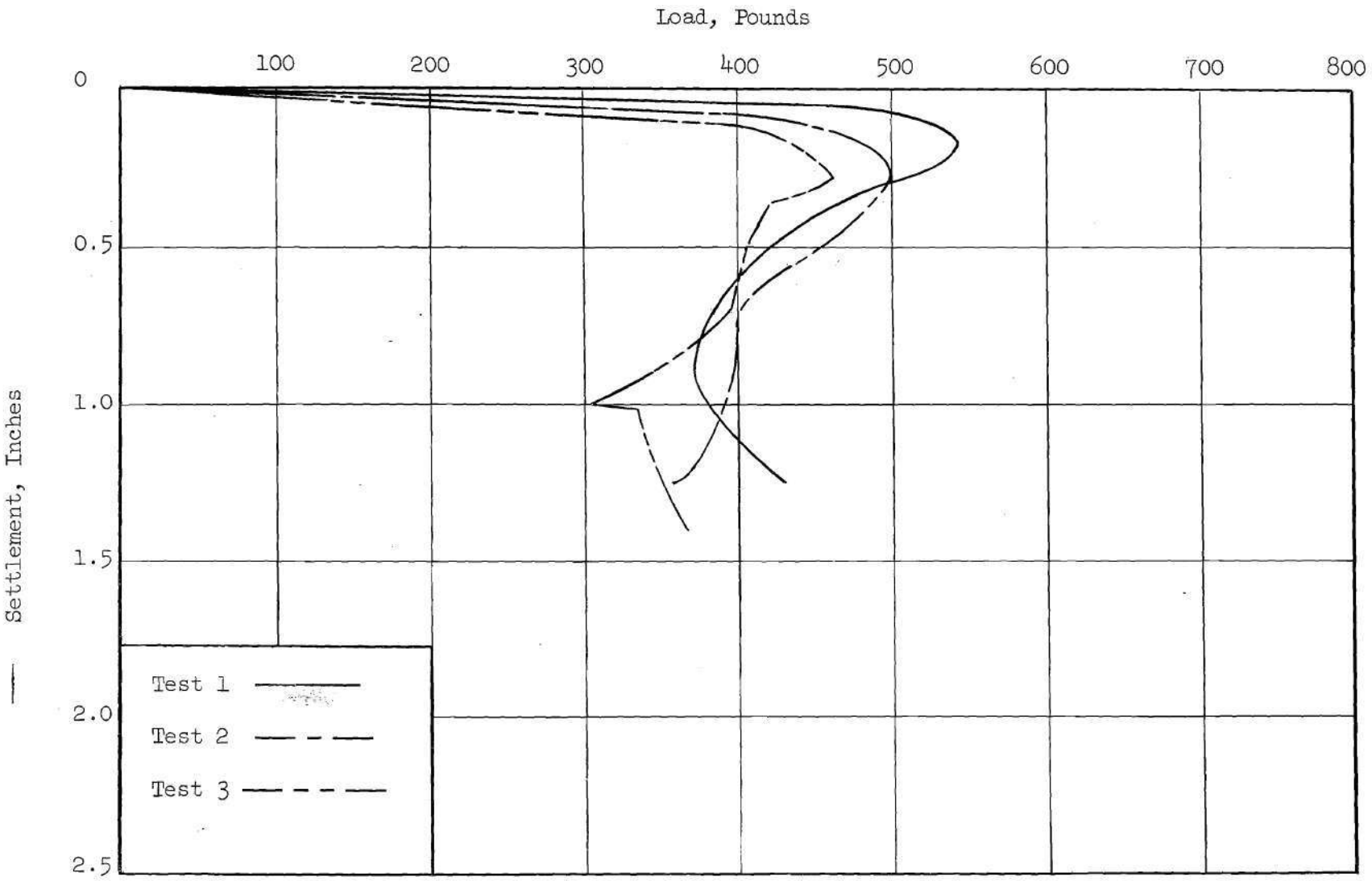

Figure 11. Load Settlement Curves

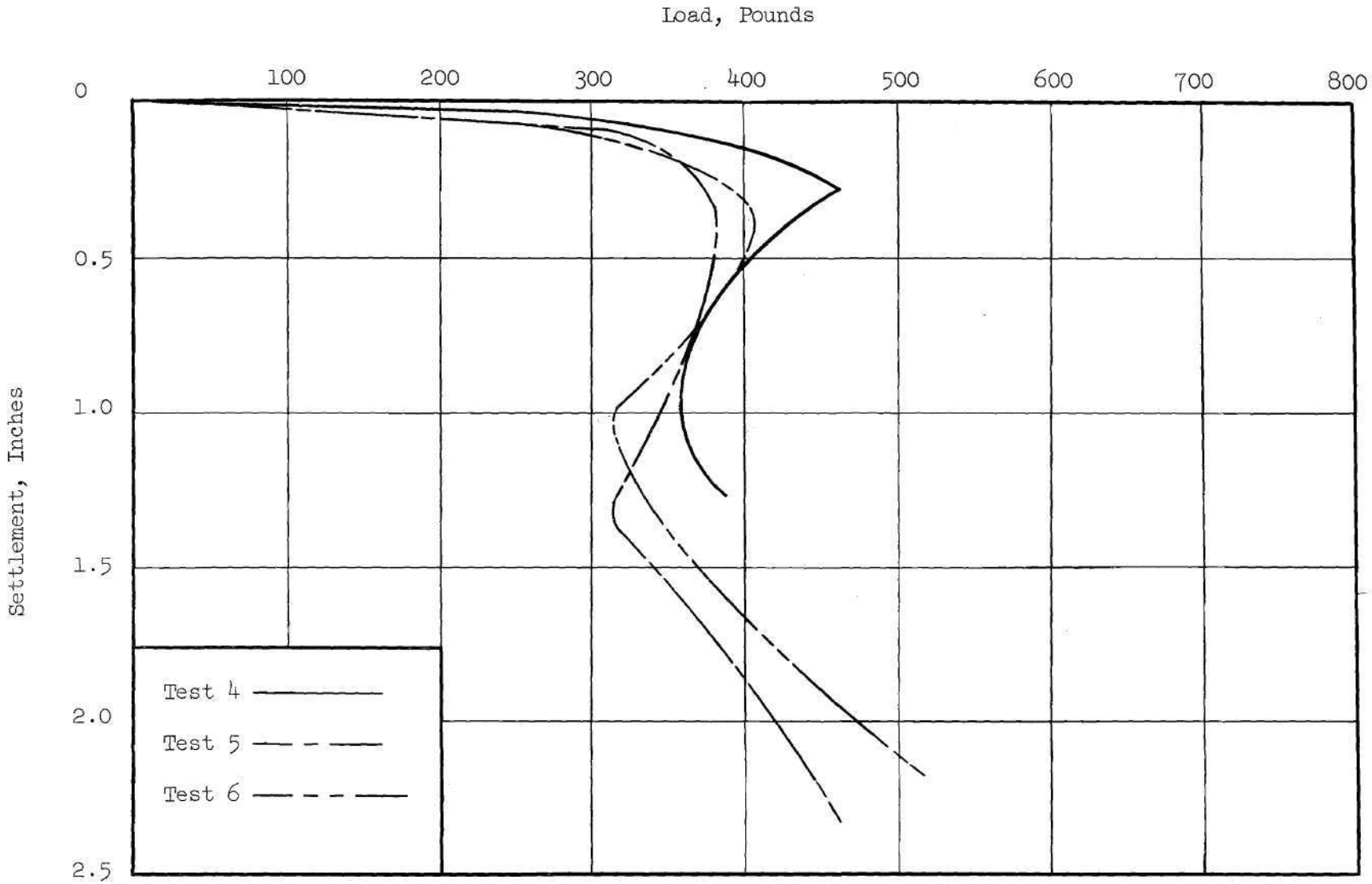

Figure 12. Load-Settlement Curves

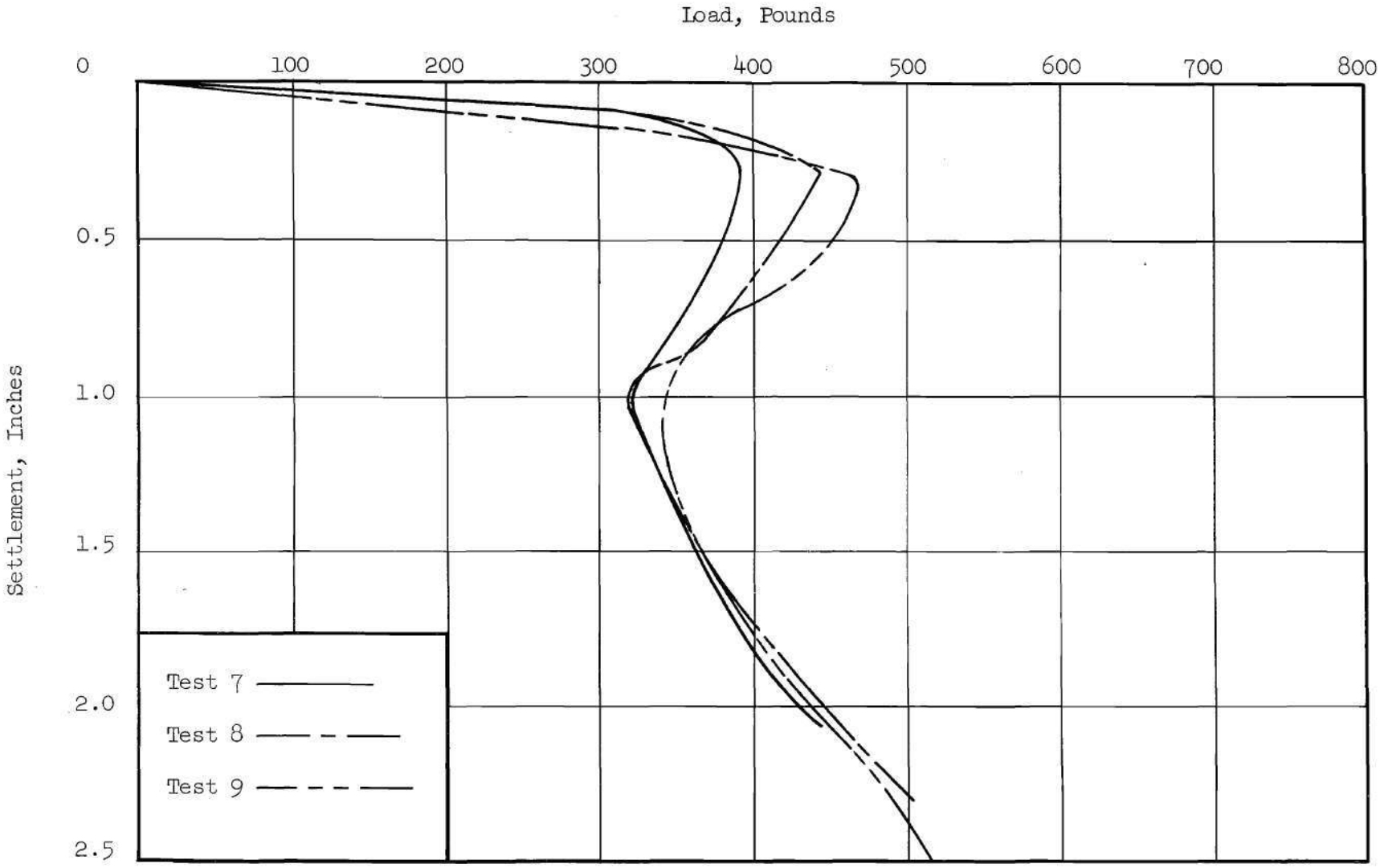

Figure 13. Load-Settlement Curves

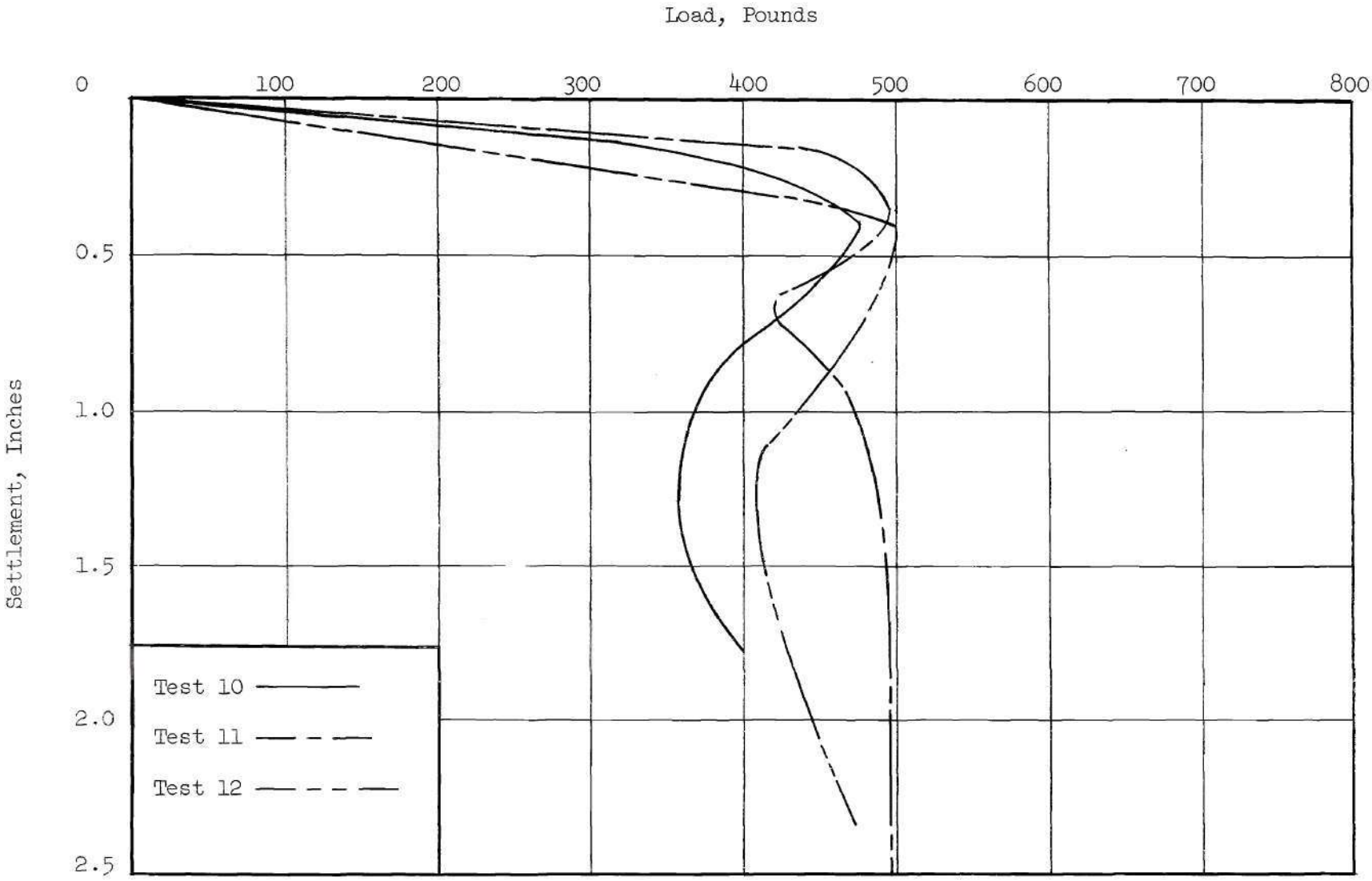

Figure 14. Load-Settlement Curves

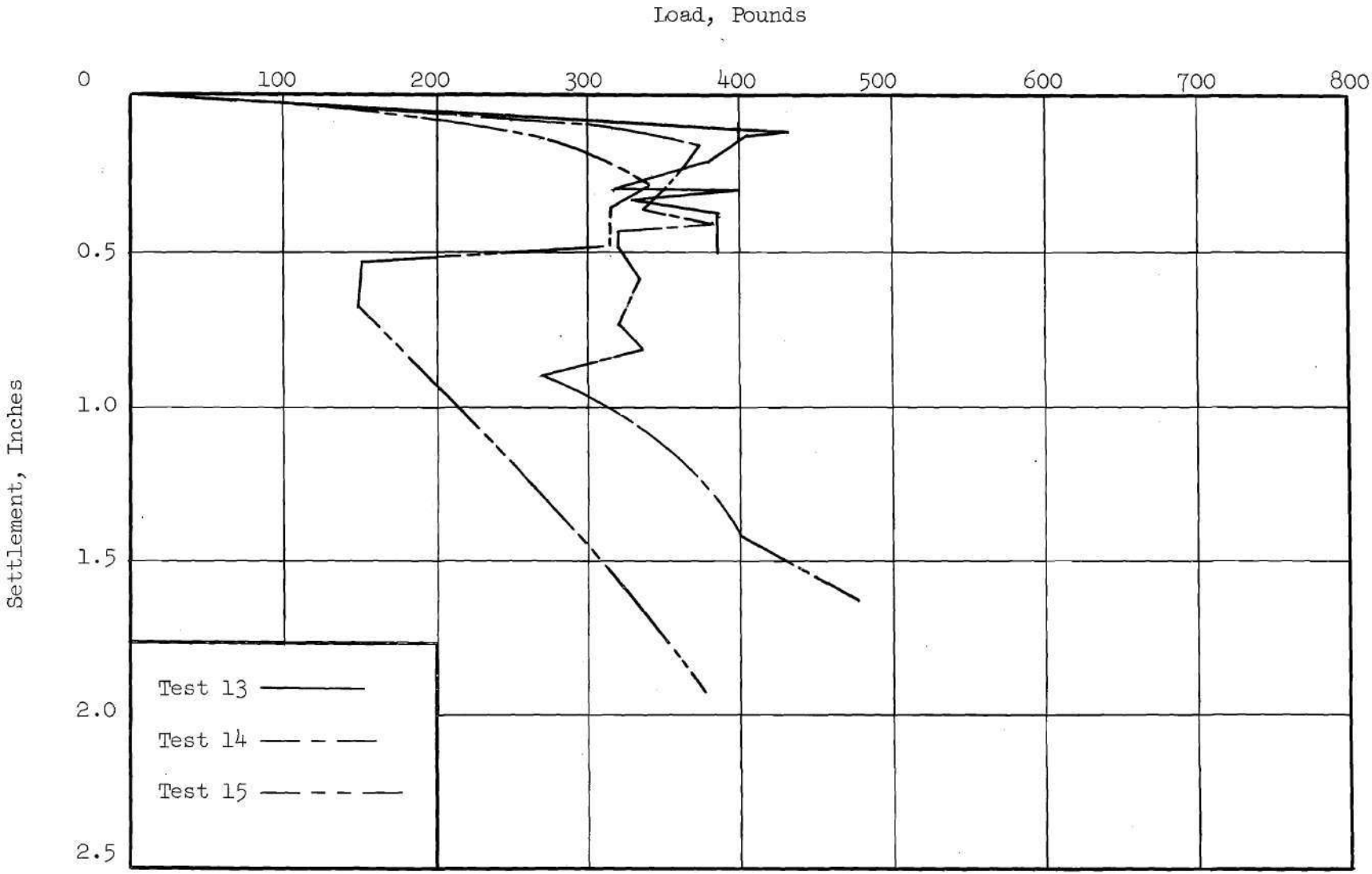

Figure 15. Load-Settlement Curves

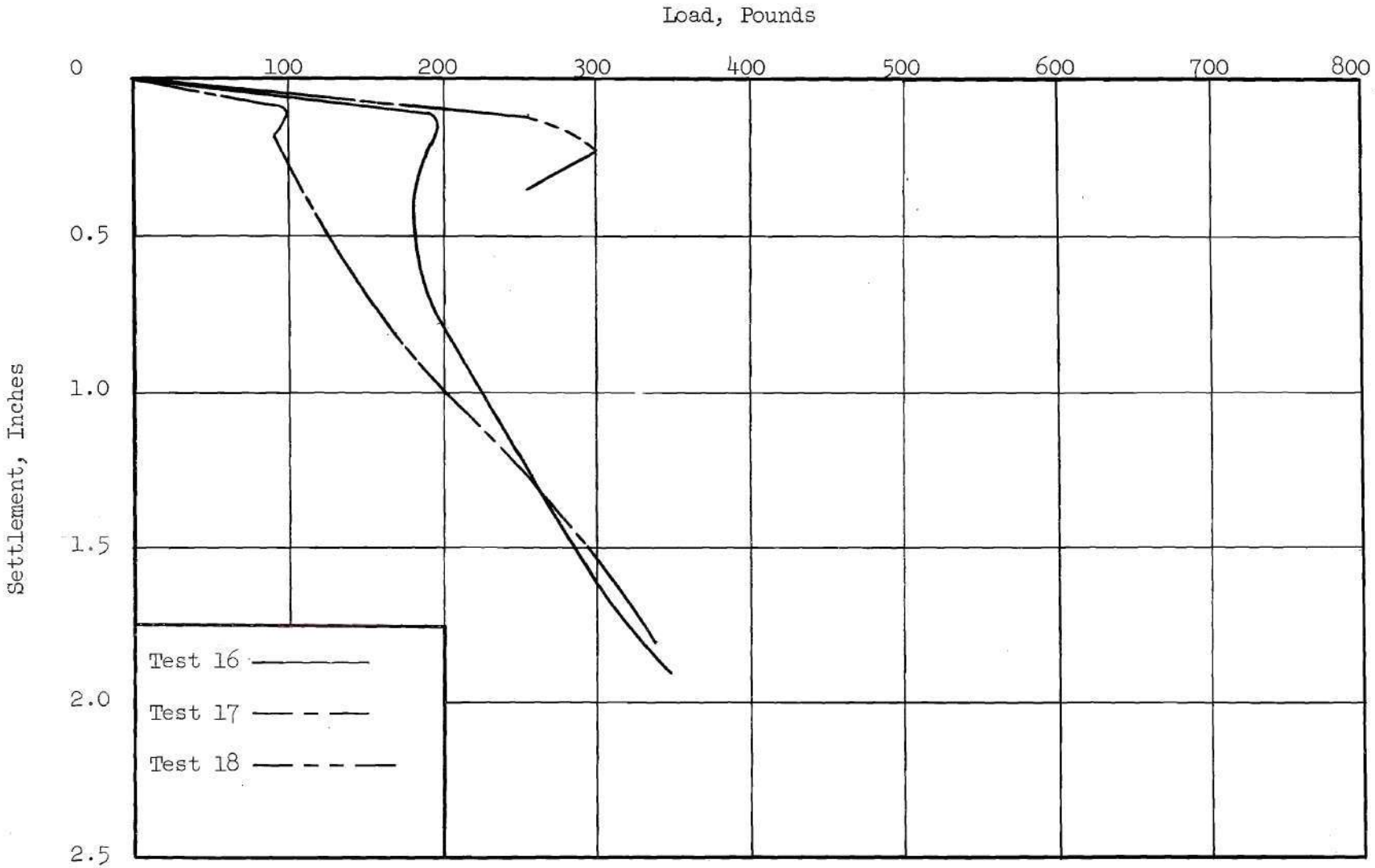

Figure 16. Load-Settlement Curves

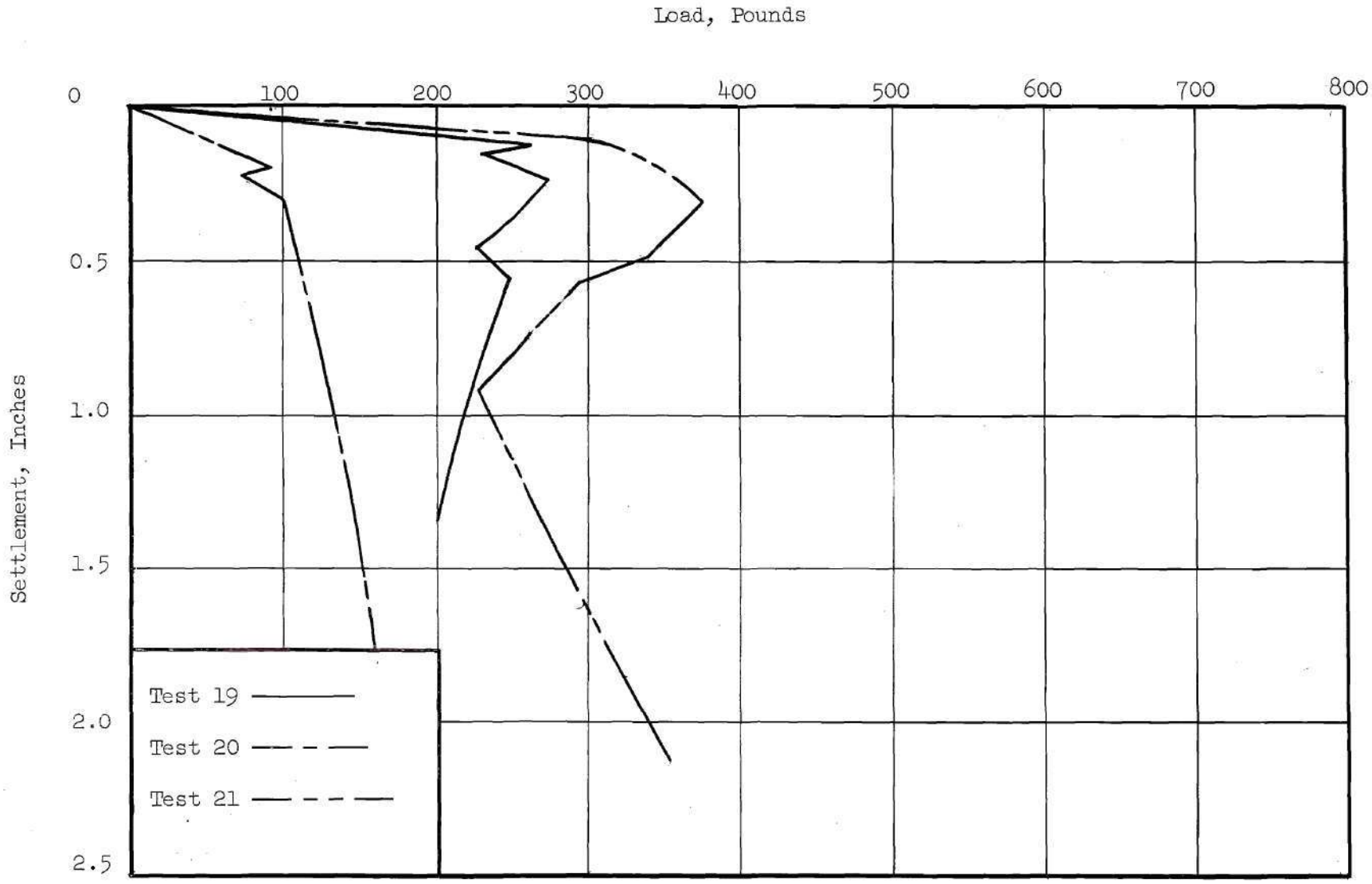

Figure 17. Load-Settlement Curves

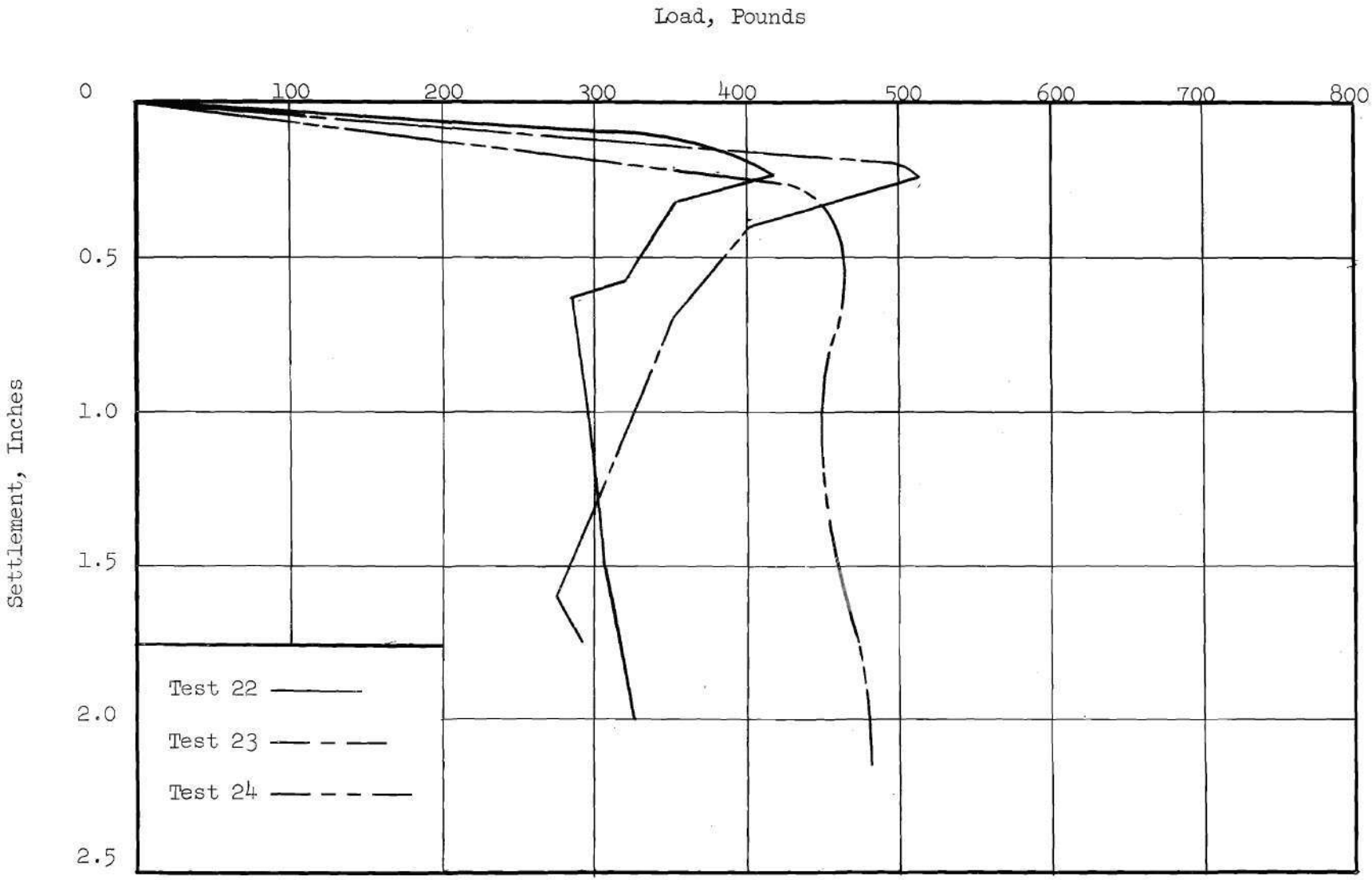

Figure 18. Load-Settlement Curves

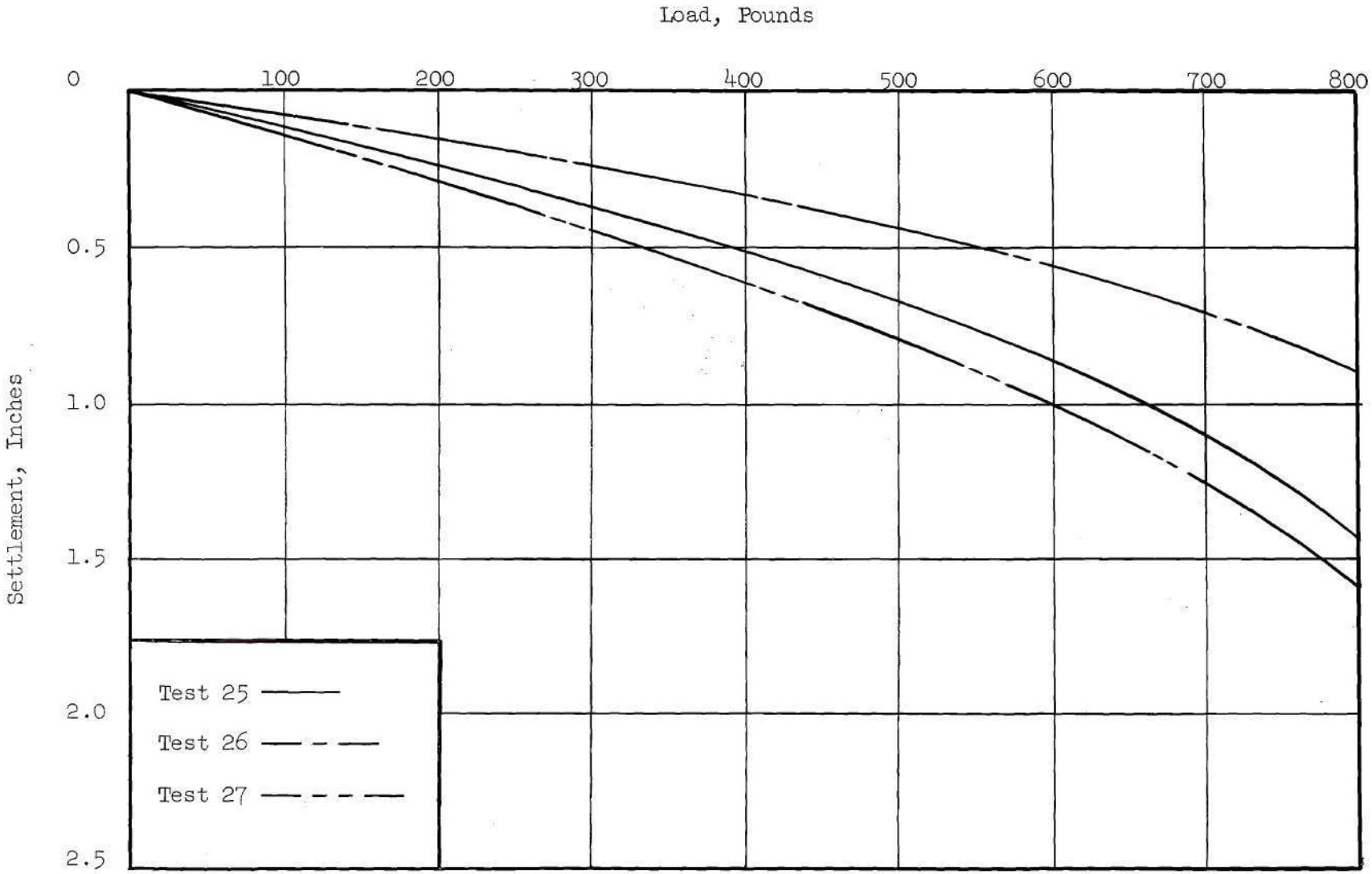

Figure 19. Load-Settlement Curves

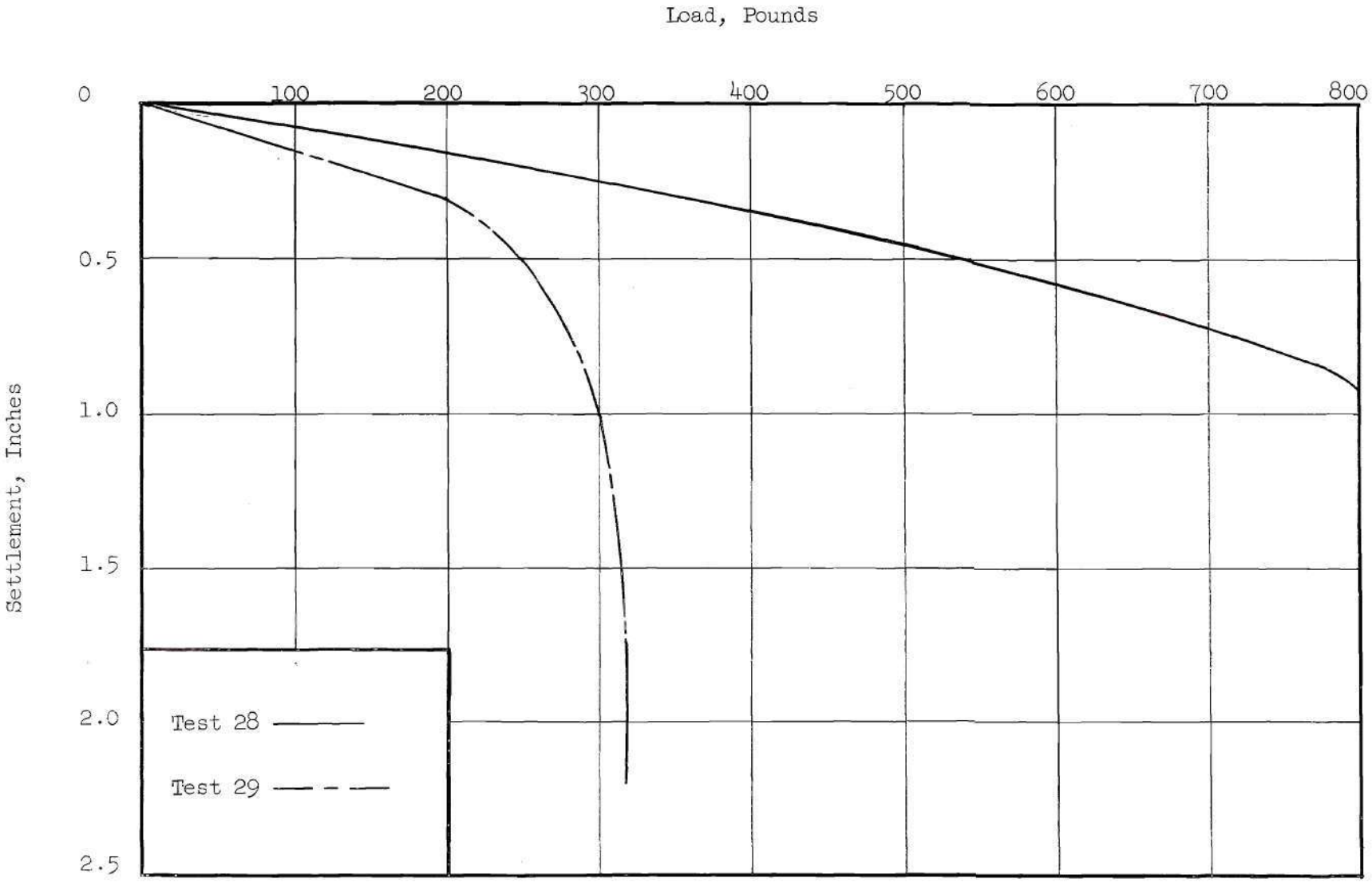

Figure 20. Load-Settlement Curves

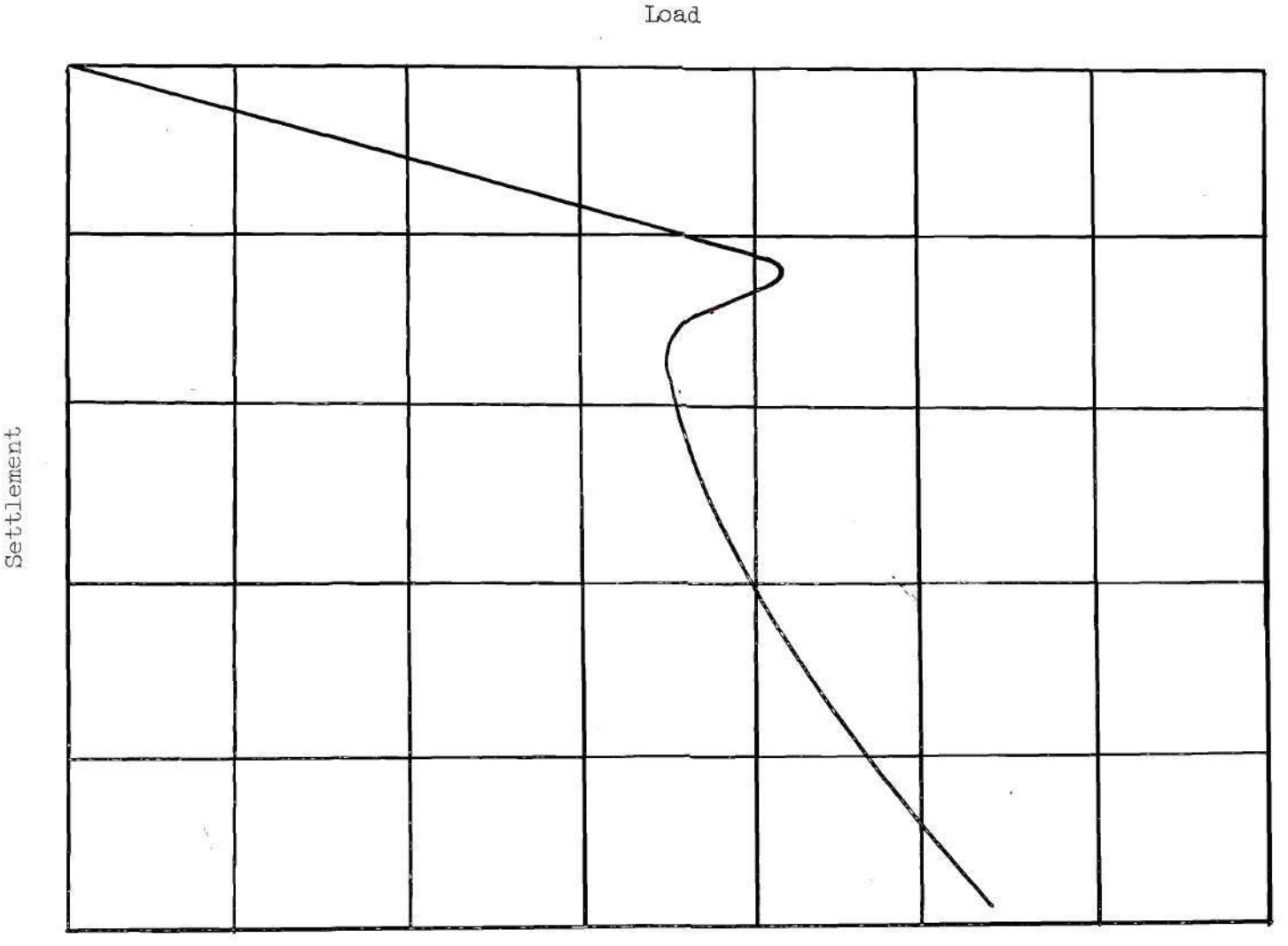

Figure 21. Typical Load-Settlement Curve for Slow Tests

as that described by DeBeer and Vesić as "punching shear" failure (7).

The load-settlement curve for this type of failure never reaches a maximum, but continues to increase at a decreasing rate. Also noticed was the fact that the walls of the depression caused by that rapid introduction of the footing into the sand stood vertically for an instant before collapsing onto the footing. This would indicate apparent cohesion resulting from negative pore-water pressure.

Table 2 summarizes the results of all tests conducted. Densities from dry tests ranged from 97.4 pounds per cubic foot to 96.6 pounds per cubic foot or a difference of 0.83 per cent. Wet test densities were slightly lower with 97.0 pounds per cubic foot as the maximum and 94.6 pounds per cubic foot the minimum or a difference of 2.54 per cent. Variations in bearing capacity due to differences in density were not corrected since the correction would not influence the general trend of results.

Figure 26 shows the relationship between rate of loading and bearing capacity for both wet and dry tests. Tests 1 through 12 were conducted with dry sand while 13 through 29 were performed on inundated sand. Excellent results were obtained for dry sand with only a very small amount of scattering. More scattering of results occurred for wet sand, but this is to be expected for this type of testing.

Both wet and dry tests produced minimum bearing capacities at 0.002 inches per second load rate. This particular critical value of load rate is not a constant for all sands, but varies depending on grain size distribution, density, and permeability of the sand used.

As the load rate increased from the minimum values obtained

Table 2. Summary of Significant Results from Load Tests

Test	Load Rate in/sec	Failure Load lb.	Settlement at Failure in.	Time to Failure sec.	$\frac{(Q_{ult})}{1/2\gamma B}$	Dry Unit Weight lb/ft^3
1	0.000023	544	0.163	7066	385	97.1
2	0.00016	495	0.263	1690	352	96.7
3	0.00030	448	0.301	1560	316	97.4
4	0.00037	464	0.279	924	328	97.4
5	0.00176	380	0.333	400	269	97.1
6	0.00203	402	0.384	194	285	97.1
7	0.00220	392	0.286	142	278	97.0
8	0.080	418	0.329	4	297	96.8
9	0.110	464	0.311	3	330	96.6
10	2.54	480	0.356	0.3	341	96.7
11	9.26	496	0.407	0.04	351	97.2
12	12.26	504	0.419	0.05	357	97.0
13	0.000096	401	0.117	2232	457	96.8
14	0.000288	380	0.156	820	435	96.5
15	0.000355	344	0.209	636	393	96.5
16	0.0020	194	0.200	106	222	95.9
17	0.0020	340	0.210	54	388	96.4
18	0.0021	300	0.279	135	342	96.7
19	0.0139	256	0.209	11.6	292	96.3
20	0.040	420	0.260	6.3	478	96.4
21	0.041	275	0.250	3.2	316	95.9
22	0.042	385	0.320	5.6	437	96.8
23	0.317	510	0.250	0.6	580	96.8
24	0.356	463	0.513	1.3	512	97.0
25	0.466	790	1.320	2.7	900	96.5
26	0.576	800	0.925	2.0	910	96.3
27	0.683	795	1.550	2.5	905	96.7
28	0.744	830	1.125	2.0	946	96.4
29	0.790	301	1.100	2.0	350	94.6

(less than 0.0001 inches per second) to the critical value of 0.002 inches per second, the bearing capacities for both wet and dry tests decreased. For wet tests, the decrease was approximately 40 per cent, while for dry tests the decrease was about 29 per cent. This drop in bearing capacity is a result of the time effect on the deformation of sands. This creep phenomenon in sands is probably the result of minute changes in particle orientation in such a way as to better resist the applied load. As the load rate increased from values less than 0.002 inches per second, the time allowed for this particle orientation is reduced and time is not allowed for the sand to build up the maximum resistance.

An increase in bearing capacity for both wet and dry tests was observed for load rates increasing from 0.002 inches per second. For dry sand, the increase was 29.0 per cent, and for saturated sand the increase was 300 per cent based on the load-failure criterion discussed previously.

In triaxial tests by Whitman (5) and Soteriades (17), an increase of shearing strength with increasing load rate was noted for dry sands. An increase of 10 to 15 per cent in strength was observed when the load rate increased from that of a normal triaxial test to rates which required only micro-seconds for the occurrence of failure. Seed and Lundgren (6) reported an increase of 15 to 20 per cent in shear strength of triaxial samples of saturated sand, neglecting the effects of dilatancy and the resulting negative pore pressure, as the load rate increased from static tests of 10 to 15 minutes duration to rapid transient load of 40 inches per second. Including dilatancy, the strength increase was found to be 40 per cent greater. The difference in the type of shear failure experienced between triaxial tests and footing tests and differences in

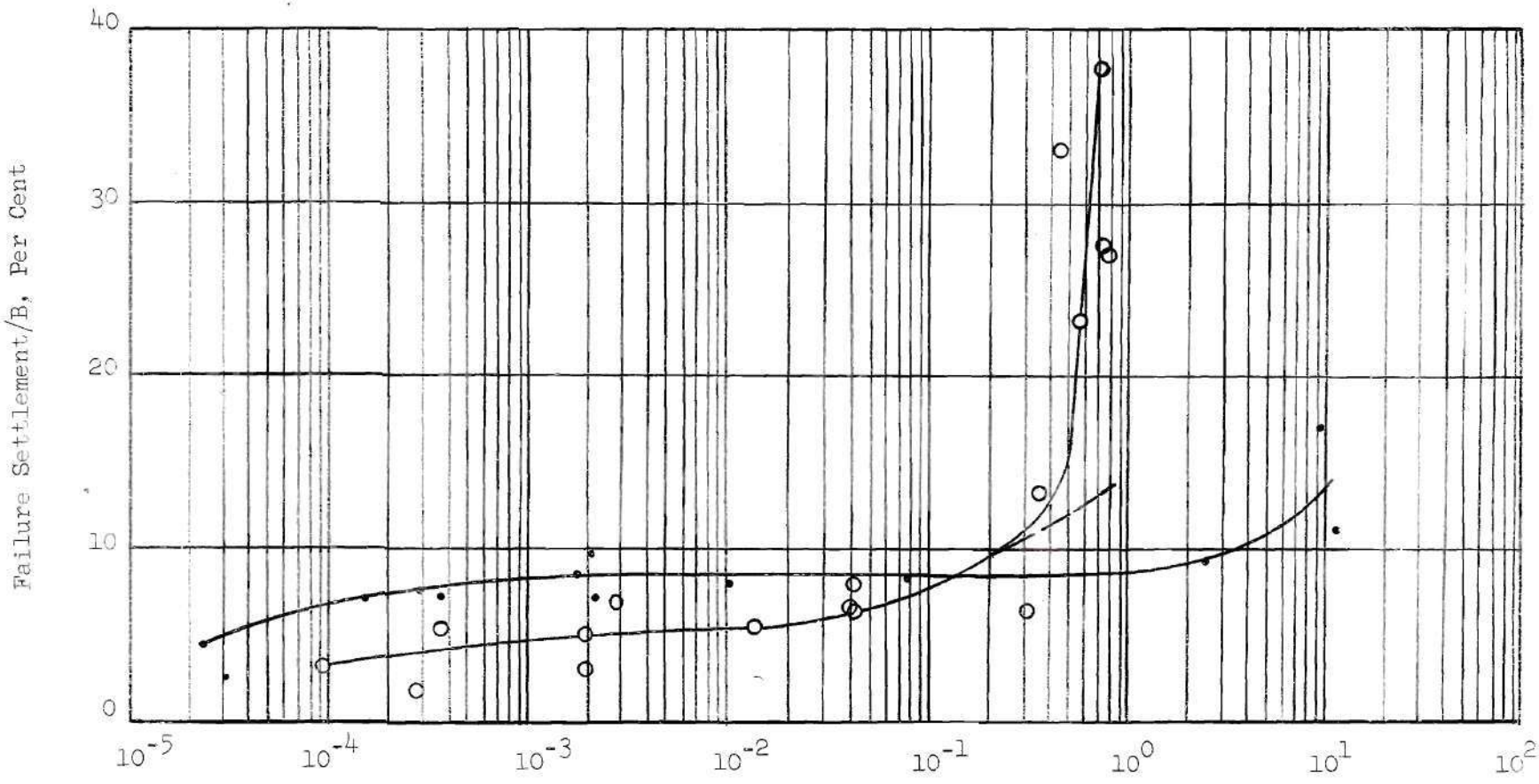

Figure 22. Variation in Per Cent Settlement at Failure with Load Rate

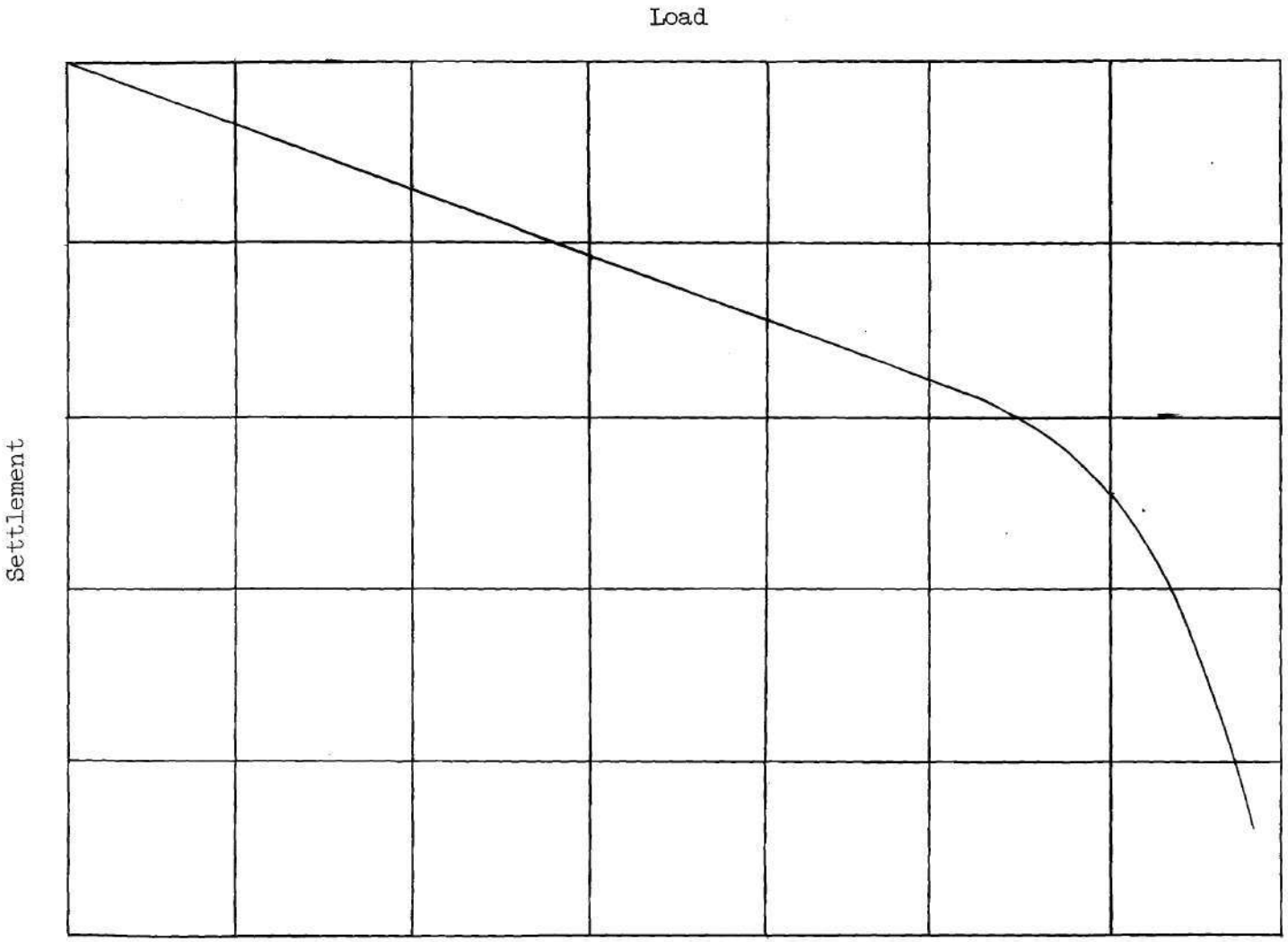

Figure 23. Typical Load-Settlement Curve for Fast Test

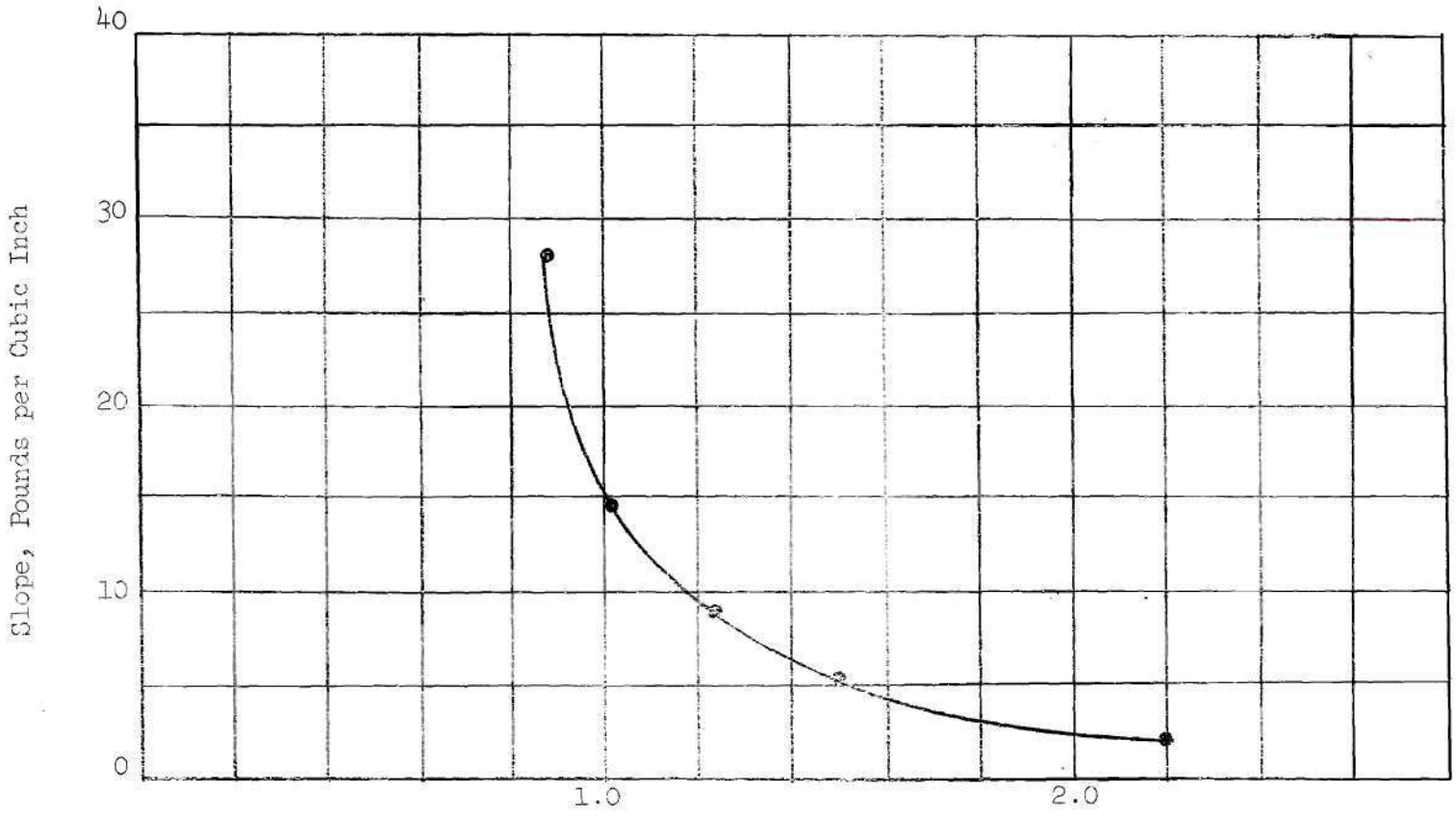

Figure 24. Plot of Slope of Load-Settlement Curve Versus Settlement for Fast Wet Tests

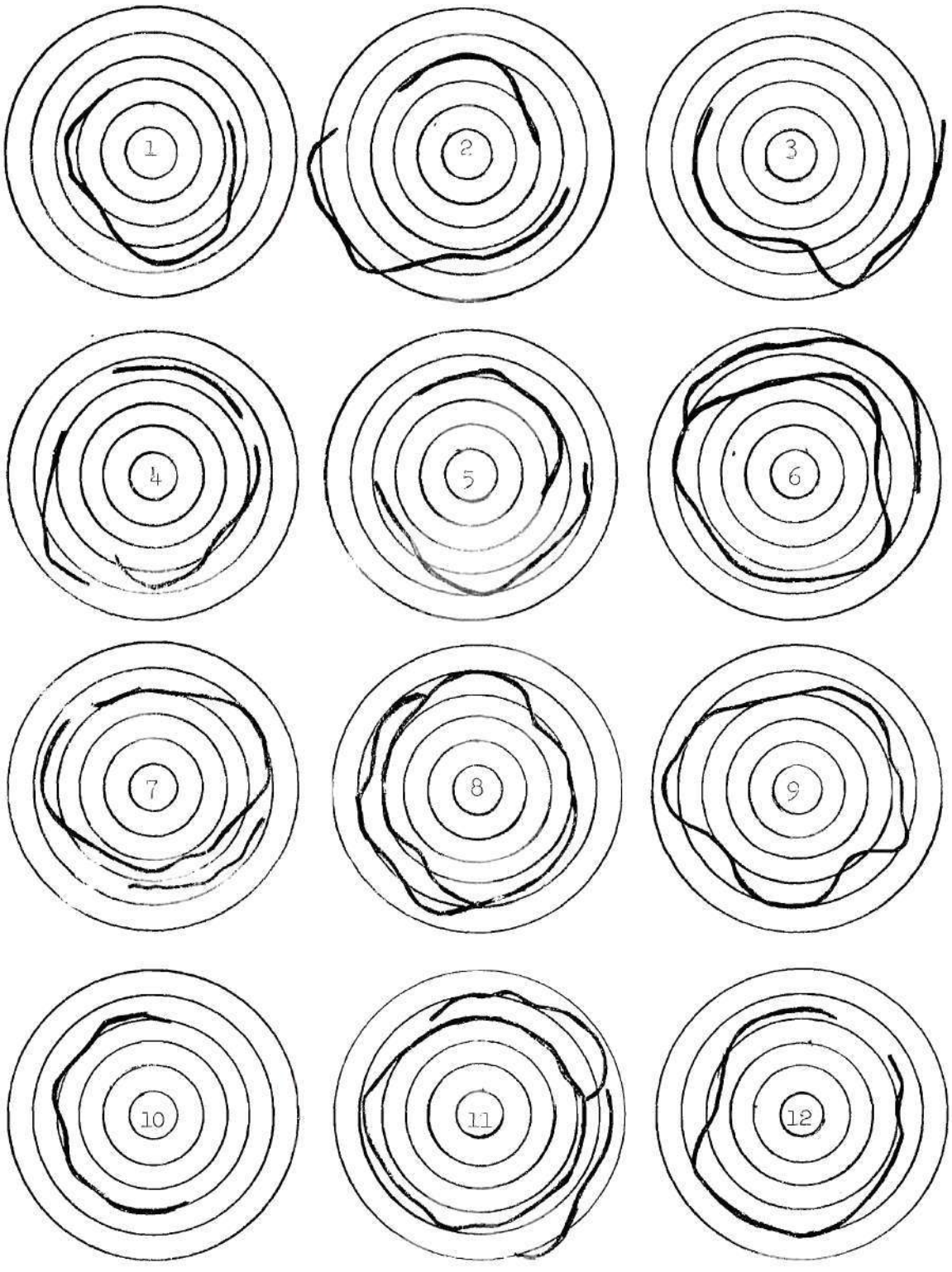

Radius of Least Concentric Circle 2 Inches.

Figure 25. Shear Surfaces

properties of the sands used by various investigators possibly explains the difference in the percentages.

The increase in shear strength with increasing load rate was explained by Terzaghi (18). Terzaghi reasoned that in rapid shear the sand grains are not allowed to follow the paths of least shearing resistance and are forced, due to lack of sufficient time, to follow shear paths which produce higher bearing capacities. This idea is supported by observations of the shear surfaces at the surface of the sand after testing. Figure 25 shows the shear surface for faster tests to be more irregular than slower tests in which the surfaces are more circular and continuous in shape.

Nash and Dixon (19), in triaxial tests on saturated sand, expressed the same idea. They reported that in rapid tests the sand particles could not adjust their positions so as to offer a minimum resistance to strain, and the structural breakdown, instead of occurring progressively, all occurred when the peak load was reached.

Pore pressures resulting from dilatancy also increased the bearing capacity as the load increased. The large increase in bearing capacity experienced in wet tests was the result of negative pore pressure produced by dilatancy. As the load rate increased, these negative pore pressures increased; their magnitude depending on load rate, void ratio and permeability of the sand. Since the void ratio, permeability and amount of dilatancy were, for all practical purposes, the same for all tests, the increase in bearing capacity was a result of negative pore pressure and strength increase due to the high rate of load. No attempt was made to determine quantitatively the magnitude of the pore pressure.

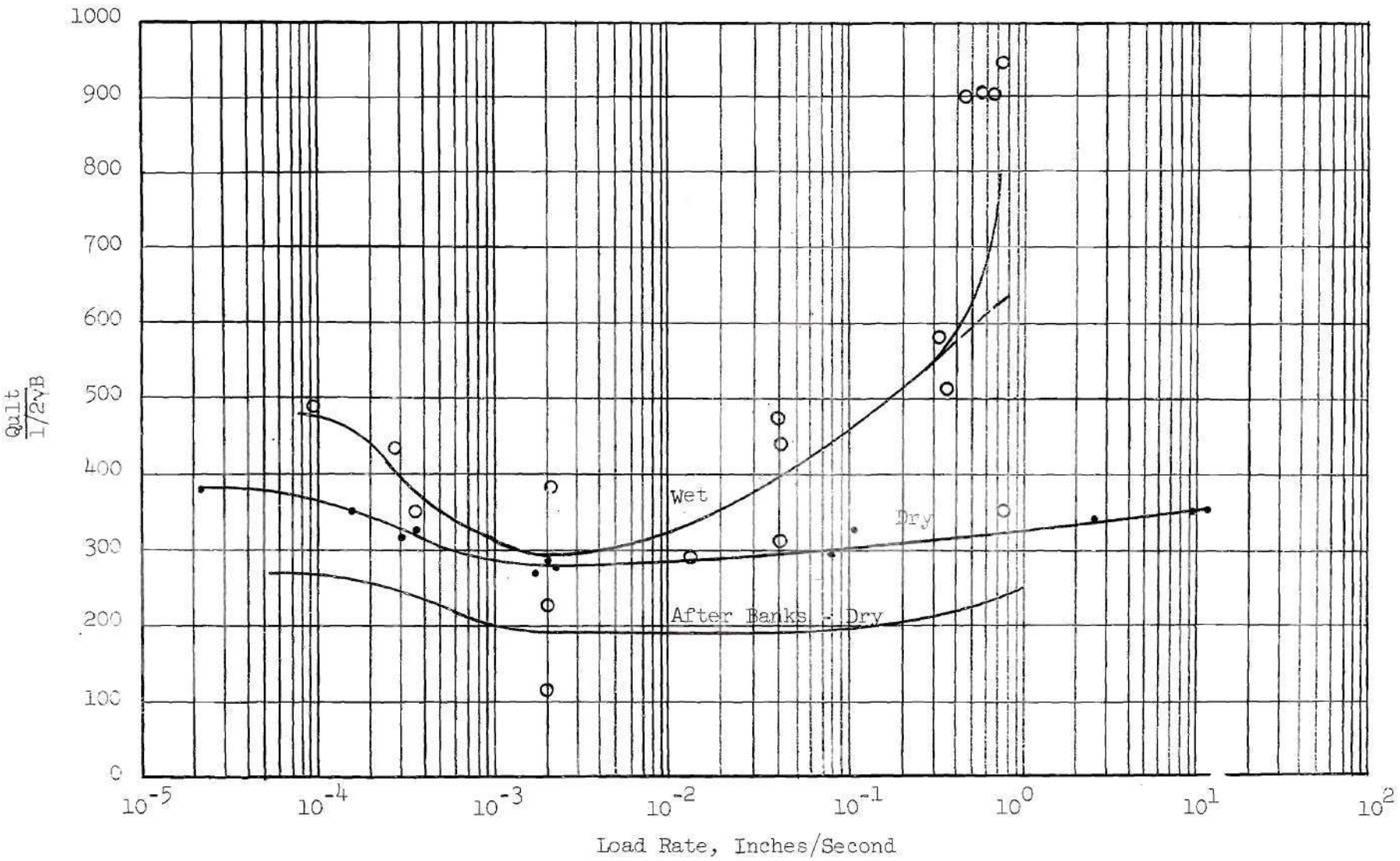

Figure 26. Bearing Capacity Factor $\left(\frac{Qult}{1/2\gamma B}\right)$ as a Function of Load Rate

Multiple failure surfaces were observed for several of the slower dry tests. However, these new shear surfaces formed after the footing had reached failure and were responsible for the gradual increase in bearing capacity after the initial failure.

Also shown in Figure 26 are the results of tests performed on the same sand by Banks (20). Shown are both his resulting plot of bearing capacity versus loading rate and points declared to be questionable as to accuracy due to the loading apparatus used. Comparing Banks' results with the author's, these questionable points are seen to be correct and Banks' plot has been extended to include these values. The average density of the author's dry tests was 97.0 pounds per cubic foot, while Banks' average density was 95.8 pounds per cubic foot. This difference in densities results in the separation of the two curves.

Of interest is the fact that, although the average density of the wet tests is 96.4 pounds per cubic foot and for the dry tests 97.0 pounds per cubic foot, the bearing capacities for the wet tests were greater. Realizing that the angle of internal friction is, for all practical purposes, identical for both dry and saturated sands, the bearing capacities of the wet tests should practically equal those of the dry tests for very slow loading rates. A difference of only 0.4 degrees in the angle of internal friction results from a difference of 0.6 pounds per cubic foot density. This seeming incongruity of results is probably due to errors and normal scattering of density data. It is easily conceivable that results of the static cone penetration method of estimating density would have a range of scattering greater than 0.6 pounds per cubic foot. Also, the method used to convert the data obtained for wet test penetrations

to the equivalent dry density could lead to some error. Another possible difference in results could be a difference in structure between the sand compacted dry and that compacted while saturated. No effort was made to determine if this structural difference existed, but it is presented here as one possibility.

Figures 27 and 28 show representative load-settlement curves for increasingly more rapid load rates of both wet and dry tests. From these curves, the modulus of deformation for both wet and dry tests is seen to decrease as the load rate increases. Vesić (7) reported the same phenomenon for similar surface footing tests. It is of interest to note that tests conducted with triaxial apparatus have produced just the opposite results. Seed and Lundgren (6) found an increase of 30 per cent in the modulus of deformation as the load rate increased from a value which produced failure in 10 to 15 minutes to 40 inches per second. Banks (20) also reported an increasing modulus of deformation with increasing load rate.

A convenient method of expressing the relationship between load and settlement is by the two constants, modulus of subgrade reaction, K, and apparent modulus of deformation, E'. Both of these terms are linear functions of the slope of the load-settlement curve. Assuming the mass of sand to be a homogeneous, isotropic, elastic solid, the relationship between E' and K may be expressed as follows:

$$E' = KBI_w$$

E' = apparent modulus of deformation, $E/(1-\nu^2)$ pounds per square inch

K = modulus of subgrade reaction, pounds per cubic inch

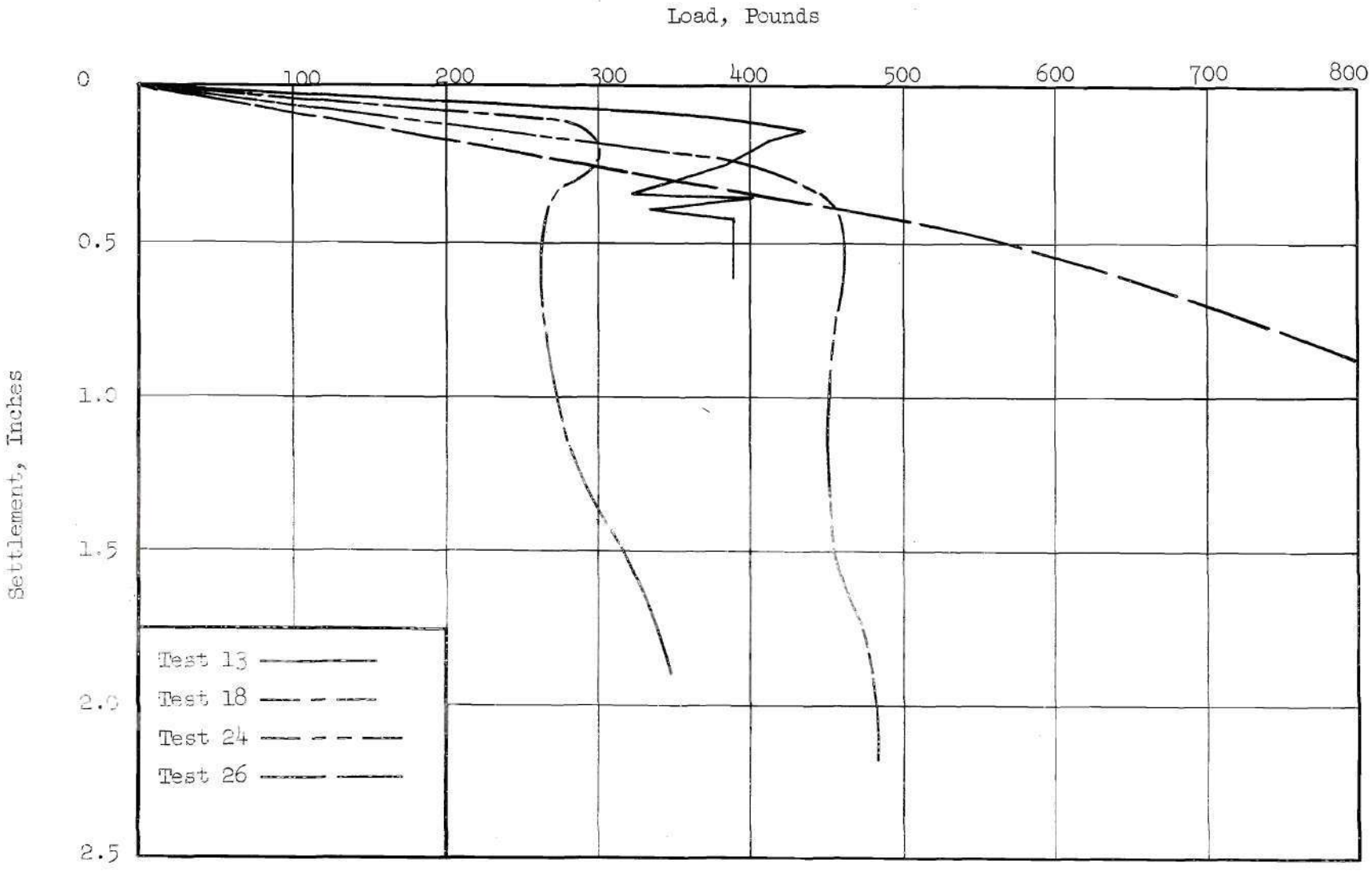

Figure 27. Typical Load-Settlement Curves for Various Load Rates for Wet Tests

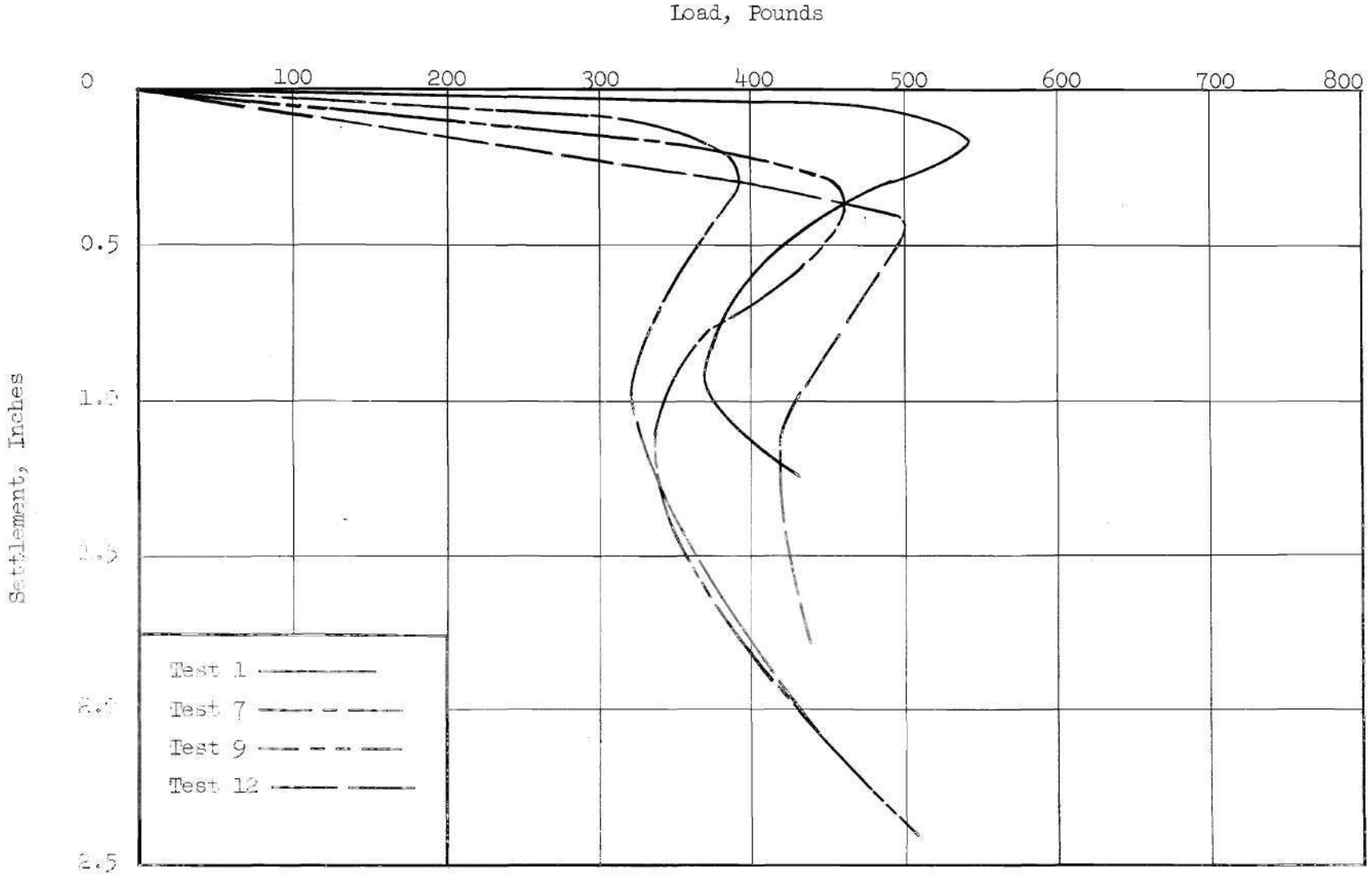

Figure 28. Typical Load-Settlement Curves for Various Load Rates for Dry Tests

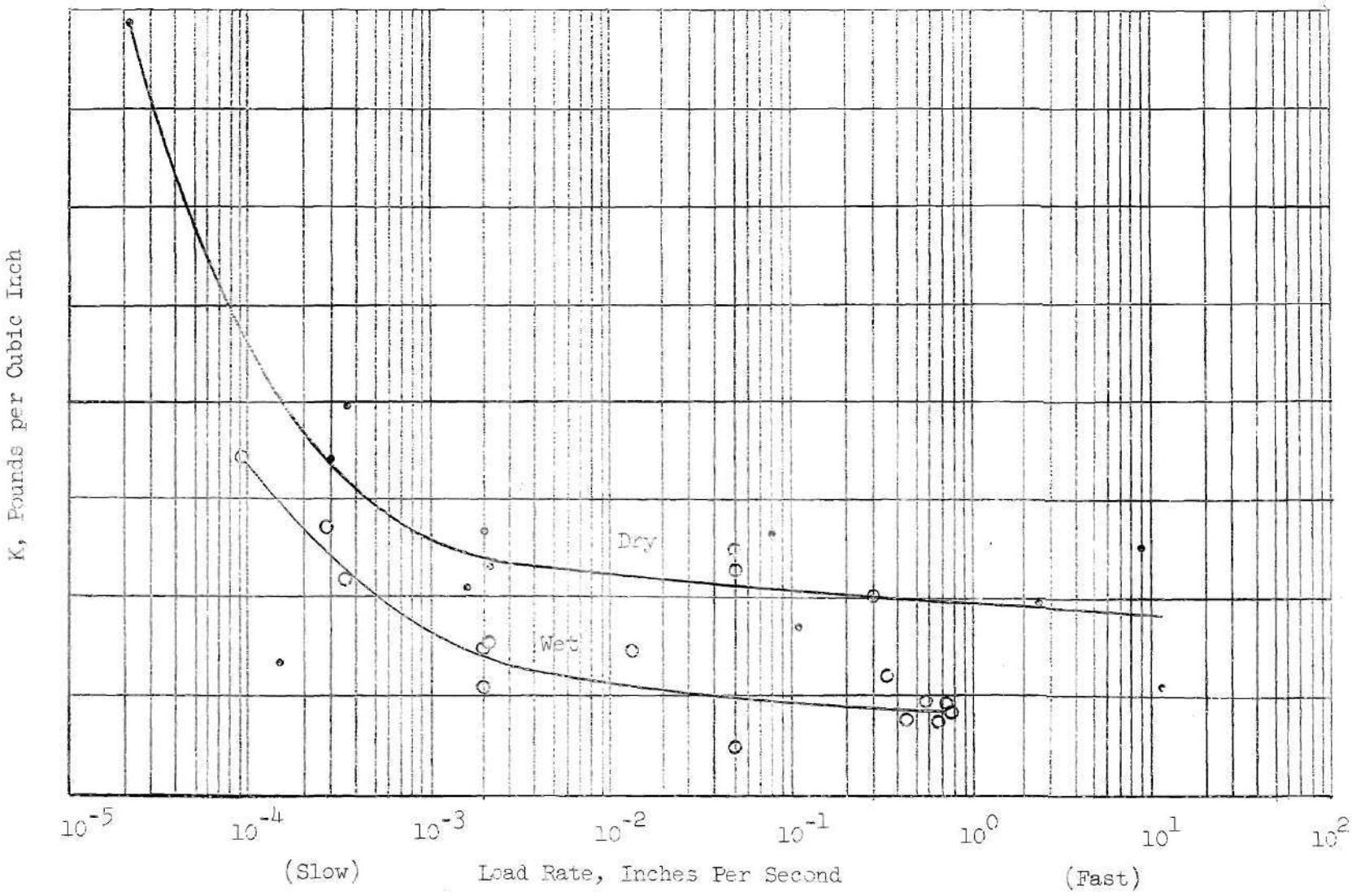

Figure 29. Modulus of Subgrade Reaction as a Function of Load Rate

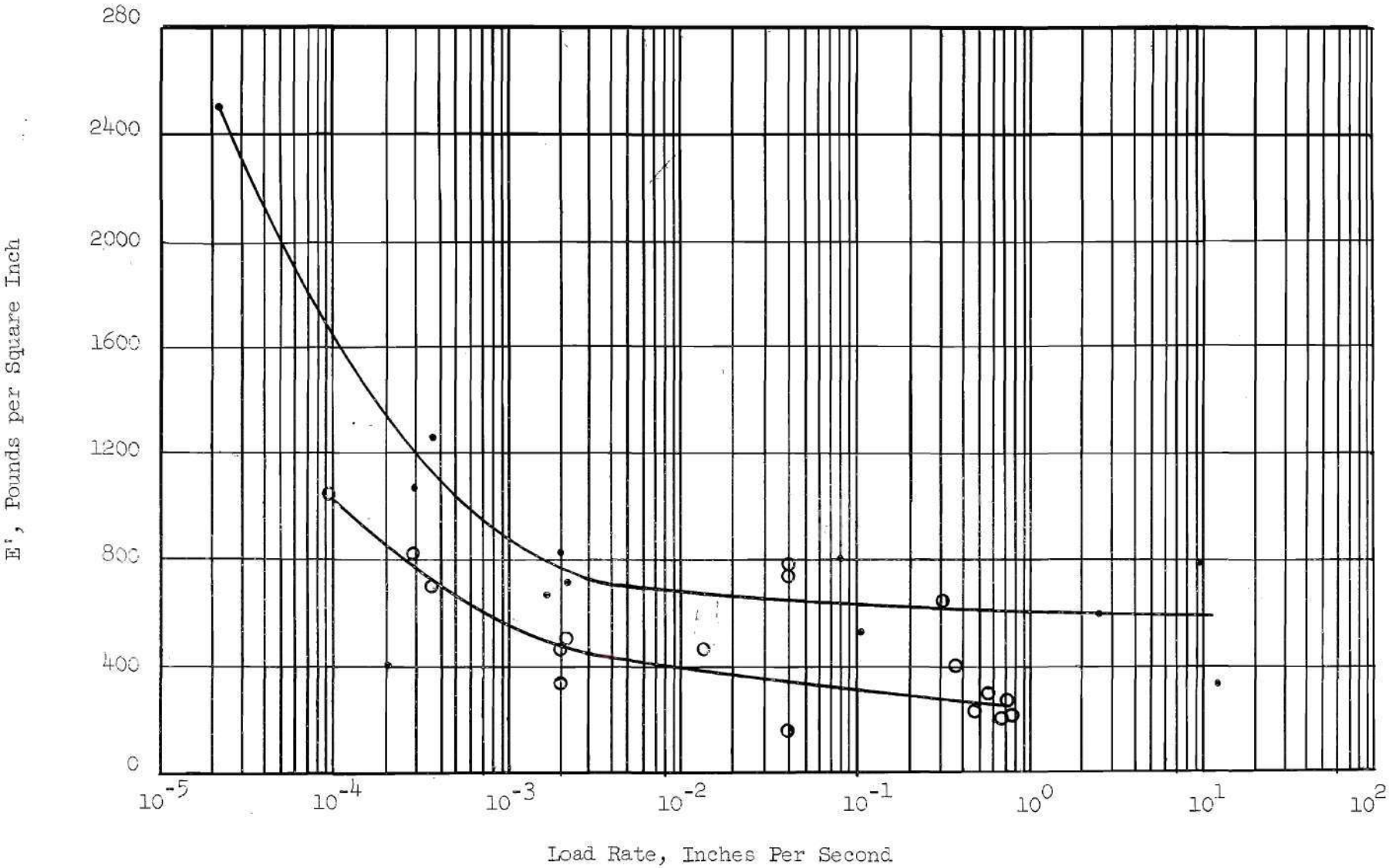

Figure 30. Apparent Modulus of Deformation as a Function of Load Rates

B = footing diameter, inches

I_w = influence factor, dimensionless, (0.785 for this investigation)

Figure 29 shows the relationship between modulus of subgrade reaction, K, and the load rate for both wet and dry tests. A continuous decrease in modulus of subgrade reaction resulted in both series of tests as the load rate increased.

Figure 30 shows the variation of the apparent modulus of deformation with load rate, uncorrected for density fluctuations.

The load-settlement curves for tests 17, 18, 27, and 28 show a zigzag variation in load occurring. As shown, the load would reach a maximum value with continuous deflection whereupon the load would suddenly drop with a corresponding increase in deflection. This same load-settlement behavior was experienced by de Josselin de Jong (21) using piles loaded in sand. The pile settlement occurred in increments with the hesitations attributed to redistributions of grain-to-grain contact.

CHAPTER IV

CONCLUSIONS

The conclusions resulting from the tests performed in this investigation are summarized as follows:

(1) An increase in the ultimate bearing capacity exists as a footing is loaded on dry or saturated sands at load rates between 0.002 inches per second and 12.3 inches per second.

(2) A decrease in the ultimate bearing capacity exists as a footing is loaded on dry or saturated sands at load rates between about 0.00005 inches per second and 0.002 inches per second.

(3) A different mode of failure exists for footings loaded at very high rates on dense, saturated sand.

(4) The modulus of subgrade reaction and the apparent modulus of deformation decrease as the load rate increases.

CHAPTER V

RECOMMENDATIONS FOR FURTHER INVESTIGATION

(1) The influence of density upon ultimate bearing capacity at various load rates should be determined.

(2) More tests should be conducted on saturated sand at this density to improve the reliability of results.

(3) Preservable models should be tested to determine the mode of failure occurring at various load rates on both dry and saturated sand.

(4) Other sizes and shapes of footings should be tested, with emphasis on larger footings.

(5) A method of measuring pore pressures while testing both saturated and dry sand should be devised.

NOTATIONS

B	Width of footing (inches)
E'	Apparent modulus of deformation (lb/in^2)
e	Void ratio
I_w	Influence Factors
K	Modulus of subgrade reaction (lb/in^3)
P	Load (lb)
Q_{ult}	Ultimate load (lb/in^2)
γ	Dry unit weight (lb/ft^3)
δ	Settlement (in)
ν	Poisson's ratio
G	Specific gravity

BIBLIOGRAPHY

1. Casagrande, A., and W. L. Shannon, "Research on Stress-Deformation and Strength Characteristics of Soils and Soft Rock Under Transient Loading," Harvard University Graduate School of Engineering Publications, No. 447, Soil Mechanics Series, No. 31, 1948.

2. Casagrande, A., and W. L. Shannon, "Strength of Soils Under Dynamic Loads," Transactions of the American Society of Civil Engineers, Vol. 114, 1949, pp. 755-772.

3. Whitman, Robert V., "Testing Soils with Transient Loads," Conference on Soils for Engineering Purposes, National University, Mexico, ASTM Special Technical Publication No. 232, Philadelphia, 1957.

4. Whitman, Robert V., "The Behavior of Soils Under Transient Loading," Proceedings of the Fourth International Conference on Soil Mechanics and Foundation Engineering, Butterworths Scientific Publications, London, 1957, Vol. 1, p. 207.

5. Whitman, Robert V., and Kent A. Healy, "Shear Strength of Sands During Rapid Loadings," Journal of the Soil Mechanics and Foundations Division, Proceedings of the American Society of Civil Engineers, Vol. 88, No. SM2, Pt. 1, April, 1962, pp. 99-132.

6. Seed, H. B., and R. Lundgren, "Investigation of the Effect of Transient Loading on the Strength and Deformation Characteristics of Saturated Sands," Proceedings of the American Society for Testing Materials, Vol. 54, 1954, pp. 1288-1306.

7. De Beer, E. E., and A. B. Vesić, "Etude expérimentale de la capacité portante du sable sous des fondations directes établies en surface," Annales des Travaux Publics de Belgique, 3, 1958, pp. 3-51.

8. Cunny, R. W., and R. C. Sloan, "Dynamic Loading Machine and Results of Preliminary Small-Scale Footing Tests," Symposium on Soil Dynamics, ASTM Special Technical Publication No. 305, Philadelphia, 1961, p. 65.

9. Cunny, R. W., and R. C. Sloan, "Static and Dynamic Behavior of Small Footings (Discussion of)," Journal of the American Society of Civil Engineers, Vol. 88, No. SM4, Pt. 1, August, 1962, p. 200.

10. Egger, W., "60 Kip Capacity Slow or Rapid Loading Apparatus," Civil Engineering Studies, Structural Research Series No. 158, Department of Civil Engineering, University of Illinois, Urbana, Illinois, June, 1957.

11. Shenkman, S., and K. E. McKee, "Bearing Capacities of Dynamically Loaded Footings," Symposium on Soil Dynamics, ASTM Special Technical Publication No. 305, Philadelphia, 1961, p. 78.

12. Selig, E. T., and K. E. McKee, "Static and Dynamic Behavior of Small Footings," Journal of the Soil Mechanics and Foundations Division, Proceedings of the American Society of Civil Engineers, Vol. 87. No. SM6, Pt.1, December, 1961, p. 29.

13. Fisher, Walter E., "Experimental Studies of Dynamically Loaded Footings on Sand," ASTIA Technical Bulletin, No. AD-290 731, July, 1962, p. 43.

14. Duncan, J. M., The Influence of Depth on the Bearing Capacity of Strip Footings in Sand, Unpublished Master's Thesis, Georgia Institute of Technology, 1962.

15. Vesic, A. S., Bearing Capacity of Deep Foundations in Sand, Paper Presented at the Annual Meeting of the Highway Research Board, Washington, D. C., January, 1963.

16. Terzahi, Karl, Theoretical Soil Mechanics, 1st ed., New York, John Wiley and Sons, Inc., 1943.

17. Soteriades, M., Stress-Strain-Time Phenomena in Sands Under Triaxial Testing Conditions, Unpublished Master's Thesis, Massachusetts Institute of Technology, 1954.

18. Terzaghi, Karl, Erdbaumechnik, Franz Deuticke, Leipzig and Wien, 1925, p. 101.

19. Nash, K. L., and R. K. Dixon, "The Measurement of Pore Pressure in Sand under Rapid Triaxial Test," Pore Pressure and Suction in Soils, Butterworths Scientific Publications, London, 1961, p. 24.

20. Banks, D. C., A Study of Bearing Capacity in Sands Under Dynamic Loading, Unpublished Master's Thesis, Georgia Institute of Technology 1962.

21. de Josselin de Jong, G., Statics and Kinematics in the Failable Zone of a Granular Material, Delft, Uitgererij Whitman, Proefschrift, Technische Hogeschool te Delft, 1959.